ACS APPLIED MATERIALS & INTERFACES

Research Article

Cite This: ACS Appl. Mater. Interfaces 2017, 9, 40031-40046

www.acsami.org

Sustained Codelivery of Cisplatin and Paclitaxel via an Injectable Prodrug Hydrogel for Ovarian Cancer Treatment

Wenjia Shen, Xiaobin Chen, Jiabin Luan, Danni Wang, Lin Yu,* and Jiandong Ding

State Key Laboratory of Molecular Engineering of Polymers, Department of Macromolecular Science, Fudan University, Shanghai 200433, China

Supporting Information

ABSTRACT: The sustained release of both the hydrophilic drug and hydrophobic drug from one delivery system remains challenging in pharmaceutics and biomaterials science. The combination of hydrophilic cisplatin and hydrophobic paclitaxel (PTX) exhibits a clinical survival advantage compared with the individual drug therapy against various tumors such as ovarian cancer. In this study, a localized, long-term codelivery system of cisplatin and PTX was developed using an injectable and thermosensitive polymer−platinum(IV) conjugate hydrogel as the carrier. The thermosensitive Bi(mPEG-PLGA)−Pt(IV) (PtGel) conjugate was synthesized via covalently linking two mPEG-PLGA copolymers onto a Pt(IV) prodrug, and its concentrated aqueous solution exhibited a reversible sol−gel transition upon heating. Meanwhile, the core−corona micelles formed by the amphiphilic conjugates in water could serve as a reservoir for the solubilization of PTX, and thus an injectable binary drug-loaded hydrogel formulation was obtained. We also found that the introduction of PTX into the conjugate hydrogel decreased its sol−gel transition temperature and improved its gel strength. In vitro release experiments showed that both of the loaded drugs were released in a sustained manner for as long as 2.5 months, which was the longest combination delivery of these two drugs ever reported. In vitro cellular assays revealed that the dual-drug system exhibited a synergistic anticancer effect against ovarian cancer cells. Finally, using the SKOV-3 ovarian cancer xenograft mouse model, we demonstrated that a single injection of the PTX-loaded conjugate hydrogel system resulted in enhanced anticancer efficacy and significantly reduced the side effects, when compared with the multiple injections of the free drug combination.

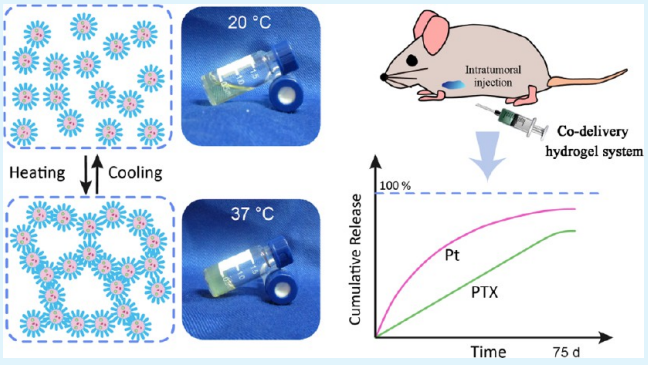

KEYWORDS: *combination therapy, cisplatin, paclitaxel, sustained drug delivery, synergistic effect, thermosensitive hydrogel*

1. INTRODUCTION

Chemotherapy is a commonly used modality for cancer therapy; however, the use of single agents is usually insufficient to achieve ideal efficacy, owing to the rapid development of drug resistance and heterogeneity in tumor.[1] Compared with the individual drug therapy, combination chemotherapy has many advantages. First, multiple drugs targeting different cellular signaling pathways can significantly improve therapeutic efficacy in synergistic ways.[2−4] Second, applying multiple drugs can modulate the genetic barriers, delay the cancer cell mutations, and thus overcome drug resistance.[3,5] Till date, hundreds of combination therapies have been explored and applied in clinical practice.[6−8]

Among them, the cisplatin + paclitaxel (PTX) association of free drugs has been become the first-line therapy for various types of cancers including non-small-cell lung cancer,[9] ovarian cancer,[6,7] cervical cancer,[10] gastric cancer,[11] breast cancer,[12,13] metastatic esophageal cancer,[14] and so on. In particular, according to the Per National Comprehensive Cancer Network guidelines, combination chemotherapy using sequential administration of PTX with a platinum-based agent is the standard of care for primary treatment of ovarian cancer. Cisplatin, a cell cycle non-specific anticancer drug, not only interacts with the nuclear DNA double helix to inhibit DNA replication and transcription but also bonds mitochondrial DNA, damages it, and generates intracellular reactive oxygen species, which leads to and accelerates cell apoptosis;[15−19] PTX is a microtubule-stabilizing agent that mainly exerts on the G_2/M phase of the cell cycle by disrupting the normal tubule disassembly required for cell division and the vital interphase process.[20,21] The coadministration of the two agents in free forms has shown good synergistic effects on cancer treatment because of their different action mechanisms and synergistic interactions. It has been reported that PTX can not only inhibit the platinum−DNA adduct repair but also increase the expression of two proapoptotic proteins Bax and Bak, which enhances the apoptosis of cisplatin-resistant tumor cells.[20,22]

Received: August 11, 2017
Accepted: October 31, 2017
Published: November 13, 2017

ACS Publications © 2017 American Chemical Society

DOI: 10.1021/acsami.7b11998
ACS Appl. Mater. Interfaces 2017, 9, 40031−40046

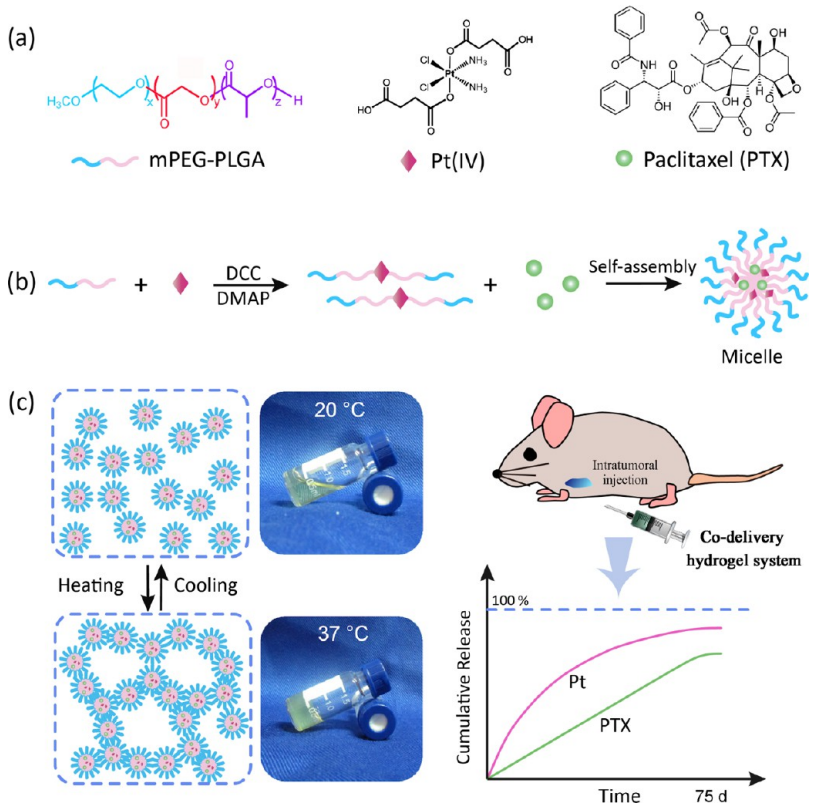

Figure 1. Design of hydrogel formulation for the combination delivery of cisplatin and PTX. (a) Molecular structures of the mPEG-PLGA diblock copolymer, Pt(IV) prodrug, and PTX. (b,c) A polymer−Pt(IV) conjugate was synthesized by covalently linking mPEG-PLGA diblock copolymers onto a Pt(IV) prodrug. The resultant conjugates could self-assemble into micelles in water and further exhibited a sol−gel transition upon heating and therefore could serve as the carrier for PTX codelivery.

It should be pointed out that both the drugs also face their own drawbacks in systemic administration: cisplatin is susceptible to be attacked by plasma proteins, leading to limited efficacy and severe side effects;[23] paclitaxel is poorly soluble in water, and its current clinical formulation contains Cremophor EL, which often causes serious hypersensitivity reactions.[21] Therefore, an important goal in the optimization of PTX−cisplatin combination therapy is to increase the drug bioavailability and accumulation in tumor tissues, while reducing the systemic toxicity simultaneously. Till date, a few nanoparticle-based delivery systems have been exploited for systemic codelivery of PTX−cisplatin, and they generally showed enhanced anticancer effects.[24−28]

Localized delivery provides another attractive option to enhance the combination therapeutic potency and minimize the drug-associated toxicities. In particular, injectable in situ forming biodegradable hydrogels have shown great potential as localized drug carriers in view of their superior advantages, including easy fabrication, target administration, less systemic side effects, as well as sustained drug release profiles.[29−40] These materials, usually in free-flowing sol states with good injectability at a low or room temperature, can conveniently encapsulate drugs through simple physical mixing; once injected into the target site, the drug-loaded systems can spontaneously turn into semisolid gels, acting as sustained release depots of drugs. As a representative type of injectable implants, thermosensitive poly(ethylene glycol) (PEG)/polyester copolymer hydrogels have been extensively utilized in the localized delivery of a variety of drugs to achieve a good target distribution and long release period.[41−49]

However, the localized, sustained codelivery of multiple drugs at the ideal dosage and the desired ratio simultaneously from one gel matrix is still very challenging, especially for two drugs with distinct chemical and physical properties, such as hydrophilic cisplatin and hydrophobic PTX. Cisplatin-loaded hydrogel formulations based on simple physical encapsulation often suffered from a burst effect, and the released period of drug just lasted a few hours.[44,50,51] By contrast, hydrophobic drugs such as PTX exhibited a sustained release from the hydrogel matrix for more than 1 month.[52]

In the present study, we developed a strategy to realize the synchronous, sustained codelivery of cisplatin and PTX in one injectable hydrogel system, and the longest combination delivery of these two drugs ever reported was achieved. A thermosensitive polymer−Pt(IV) conjugate, Bi(mPEG-PLGA)−Pt(IV) (PtGel), was synthesized via covalently linking the hydrophobic ends of two mPEG-PLGA diblock copolymers onto a Pt(IV) prodrug, which can be reverted to cisplatin upon intracellular reduction.[53−55] The amphiphilic conjugates can self-assemble into core−corona micelles in the aqueous medium, and its concentrated solution exhibits a reversible sol−gel transition as the temperature increases. This system not only increased the solubility of hydrophobic PTX by incorporating it into the hydrophobic inner cores but also served as its long-acting delivery carrier. Thus, a promising codelivery hydrogel system for cisplatin and PTX was achieved, as illustrated in Figure 1. We carried out the corresponding chemical synthesis and material preparation and then examined the temperature-responsive gelation properties and micellelization behavior of this conjugate aqueous system with or without

DOI: 10.1021/acsami.7b11998
ACS Appl. Mater. Interfaces 2017, 9, 40031−40046

PTX. Furthermore, we demonstrated the long-acting release characteristics of Pt and PTX codelivery and their synergistic effect against SKOV-3 cells. Finally, we determined the in vivo synergistic antitumor efficacy of this dual-drug-loaded hydrogel system in ovarian tumor-bearing nude mice models.

2. MATERIALS AND METHODS

2.1. Materials. Methoxyl poly(ethylene glycol) [mPEG with molecular weight (MW) 750], PEG with MW 1500, stannous octoate [$Sn(Oct)_2$] of purity 95%, 4-dimethylaminopyridine (DMAP), dicyclohexylcarbodiimide (DCC), and hexamethylene diisocyanate (HMDI) were purchased from Sigma-Aldrich. D,L-Lactide (LA) and glycolide (GA) were purchased from Jinan Daigang Biomaterial Co., Ltd (China) and used as received. Cisplatin (99.6%) was purchased from Shandong Boyuan Pharmaceutical Co., Ltd (China). PTX was provided by Shanghai Meishidun Biotechnology Co., Ltd (China). PTX Injection (Taxol) for clinical usage was obtained from the Obstetrics and Gynecology Hospital of Fudan University and produced by Qingdao Jinfeng Pharmaceutical Co., Ltd (China). Dimethyl sulfoxide (DMSO) and dimethylformamide (DMF) were dehydrated with CaH_2 and purified via reduced-pressure distillation. Other reagents were used without further purification.

2.2. Synthesis of Bi(mPEG-PLGA)−Pt(IV) (PtGel) Conjugate. *2.2.1. Synthesis of mPEG-PLGA Diblock Copolymer.* mPEG-PLGA diblock copolymers were synthesized via ring-opening polymerization of LA and GA in the presence of mPEG as the macroinitiator and $Sn(Oct)_2$ as the catalyst.[56] Briefly, mPEG (15.0 g, 0.02 mol) was dried in a three-neck flask under vacuum at 130 °C for 3 h to remove the residual moisture from the polymer. Then, LA (28.2 g, 0.39 mol) and GA (3.8 g, 0.065 mol) were added into the flask and stirred under reduced pressure at 100 °C for 30 min. After 40 mg of $Sn(Oct)_2$ was added, the reaction system was heated to 150 °C and stirred under argon protection for 12 h. The crude products were washed using 80 °C water four times to remove the unreacted monomers and low-MW products and then lyophilized to eliminate the residual water. The final products were collected and stored at −20 °C until use, and the yield was 70%.

2.2.2. Synthesis of cis,cis,trans-$Pt(NH_3)_2Cl_2(OOCCH_2CH_2COOH)_2$. The dicarboxyl Pt(IV) compound was synthesized according to the previous publications.[54,57] First, cisplatin was oxidized by 30% H_2O_2 in the dark (70 °C, 2 h) to *cis,cis,trans*-$Pt(NH_3)_2Cl_2(OH)_2$ in 78% yield. Then, two carboxyl groups were introduced onto *cis,cis,trans*-$Pt(NH_3)_2Cl_2(OH)_2$ by reacting it with succinic anhydride in anhydrous DMSO at 70 °C for 24 h in the dark under an argon atmosphere. A pale yellow powder *cis,cis,trans*-$Pt(NH_3)_2Cl_2(OOCCH_2CH_2COOH)_2$ was obtained in 65% yield after freeze-drying and recrystallization from acetone.

2.2.3. Synthesis of Bi(mPEG-PLGA)−Pt(IV) Conjugate. mPEG-PLGA (8.3 g, 3.1 mmol) was dissolved in 100 mL of toluene and heated to a azeotropy state to remove the residual water from the polymer. After the remaining toluene was further removed via rotary evaporation, the polymers were redissolved in 18 mL of anhydrous DMF; then, *cis,cis,trans*-$Pt(NH_3)_2Cl_2(OOCCH_2CH_2COOH)_2$ (0.96 g, 1.8 mmol), DCC (1.30 g, 6.3 mol), and DMAP (0.77 g, 6.3 mol) were added and stirred at room temperature away from light under an argon atmosphere for 48 h. After the completion of the reaction, a few drops of water were added to turn extra DCC into insoluble *N,N′*-dicyclohexylurea (DCU), which was then removed by filtration. The crude products were precipitated by ethyl ether under −20 °C and dialyzed against deionized water for 12 h and finally lyophilized to obtain the final product in 65% yield.

2.2.4. Synthesis of ABA or BAB-Type of PEG/PLGA Triblock Copolymers. BAB-type triblock copolymer mPEG-PLGA-mPEG (PELE) as a control polymer was synthesized via coupling reaction of mPEG-PLGA diblock copolymers using HMDI as the coupling agent.[56] Briefly, mPEG-PLGA (5.3 g, 2 mmol) was dissolved in toluene and heated to remove the residual moisture from the polymer by azeotropic distillation. Next, HMDI (0.18 g, 1.05 mmol) and $Sn(Oct)_2$ (10 mg) were added to the mixture, and the reaction system was heated to 60 °C and stirred for 6 h. The products were precipitated with ethyl ether and washed with 80 °C water and then lyophilized in 78% yield. Another ABA-type PLGA−PEG−PLGA (PLEL) triblock copolymer with a similar PEG−PLGA block ratio and LA/GA molar ratio was synthesized by a similar protocol as described in 2.2.1 but using PEG 1500 as the macroinitiator, and the yield of products was 85%.

2.2.5. Physical−Chemical Characterization. Proton nuclear magnetic resonance (^{1}H NMR) spectra were recorded on a 400 MHz proton FT-NMR spectrometer (AVANCE III HD, Bruker) using tetramethylsilane as the internal standard and DMSO-d_6 or $CDCl_3$ as the solvent. MWs and their distributions of synthesized polymers were confirmed on a gel permeation chromatography apparatus (GPC, Agilent 1260) with DMF as the eluent solvent at a flow rate of 1.0 mL/min at 50 °C, and monodispersed polymethylmethacrylates standards were used for calibration. Platinum (Pt) content of the PtGel conjugate was determined by inductively coupled plasma optical emission spectrometry (ICP−OES, Hitachi P-4010) at the spectral line of 265.945 nm based on the standard curve of Pt.

2.3. Sol−Gel Transition. The tube-inverting method was used to determine the sol−gel transition temperature of polymer aqueous solution.[58−60] Briefly, 0.5 mL of polymer solution was injected into 2 mL vials and equilibrated at 4 °C overnight. Next, the vials containing the samples were immersed in a water bath at a given temperature for 10 min and then inverted 180°. If no visible flow was observed within 30 s, the sample was considered as a gel. Observation was conducted from 20 to 60 °C with an increment of 1 °C each step.

Dynamic rheological properties of polymer solutions were investigated using a dynamic stress-controlled rheometer (Kinexus, Malvern) with a cone plate (diameter: 60 mm, cone angle: 1°). A thin layer of low-viscosity silicon oil was added onto the cone fringe to minimize water evaporation. The time sweep measurements were performed at an oscillation frequency of 10 rad/s with a heating rate of 0.5 °C/min, which was controlled by a Peltier temperature controller.

2.4. Preparation of PTX-Loaded Hydrogel Formulation. PTX-loaded hydrogel formulations were prepared by a two-step method. PTX and polymers were first mixed and dissolved in acetone. Next, acetone was removed by rotary evaporation and lyophilization. The well-dispersed drug−polymer mixture was redissolved in deionized water at 4 °C to form a homogeneous solution and then stored at −20 °C before use. The sol−gel transition behavior of the drug-loaded hydrogel formulation was studied using the same method as described in section 2.3.

2.5. Studies of Micellization. *2.5.1. Dynamic Light Scattering (DLS).* The sizes of micelles formed in polymer aqueous solutions and their distributions were measured on a nanoparticle analyzer (Zetasizer Nano, ZS90, Malvern) as a function of temperature. The light scattering angle was set as 90°. Before measurements, the samples were filtered through 0.45 μm filters to remove possible dust. The hydrodynamic diameter (D_h) of particles was calculated based on the Stokes−Einstein equation.

2.5.2. Transmission Electron Microscopy (TEM). Microscopic images of micelles of the polymer solutions with or without PTX were obtained by TEM (Tecnai G2 20 TWIN, FEI). Sample solutions (20 μL, 1 wt % polymer) were dropped on a copper grid coated with a thin carbon film and dried under an infrared lamp and observed under an accelerating voltage of 200 kV.

2.5.3. Critical Micelle Concentration (CMC). The CMC of the polymer aqueous solutions with or without PTX was determined using a hydrophobic dye, 1,6-diphenyl-1,3,5-hexatriene (DPH), as the probe.[56] A series of polymer solutions with gradient concentrations from 0.002 to 0.1 wt % were prepared at 4 °C. Then, DPH solution (0.4 mM in methanol) at the ratio of 10 μL/mL was added to the polymer solutions, and the mixtures were stored under 4 °C overnight. The ultraviolet (UV) absorbance at 320−420 nm was scanned using an ultraviolet−visible (UV−vis) spectrometer (TU 1950, Persee General) after equilibration of samples at 20 °C for 4 h. The difference of absorbance at 377 and 400 nm was plotted versus the logarithmic

DOI: 10.1021/acsami.7b11998
ACS Appl. Mater. Interfaces 2017, 9, 40031−40046

polymer concentration, and the CMC values were calculated accordingly.

2.6. In Vitro Drug Release. PtGel conjugate solution and PTX-loaded polymer or conjugate solutions (25 wt %, 0.5 mL) were injected into 15 mL vials and equilibrated at 4 °C overnight and then incubated in a shaking bath (37 °C, 50 rpm) for 15 min to allow gelation. Phosphate-buffered solution (PBS, 10 mL, pH 7.4, containing 0.5 wt % Tween 80 and 0.025 wt % NaN_3) was gently added to each vial as the release medium. At scheduled time intervals, 9 mL of medium was withdrawn and then replaced with 9 mL of fresh medium. The Pt amount in the release medium was determined by ICP−OES. For the analysis of the PTX content, a given amount of the collected release medium was lyophilized and then redissolved in acetonitrile before measurement on a high-performance liquid chromatography (HPLC, Waters e2695) instrument that was equipped with a C18 column (SunFire, 4.6 × 150 mm, 5 μm) and a UV detector (Waters 2489). The mobile phase was acetonitrile/water (v/v = 50/50) at a flow rate of 1.0 mL/min, and UV absorbance was detected at a wavelength of 227 nm under 25 °C. The cumulative release amount of the two drugs was calculated from the calibration curve accordingly.

The release profiles of Pt and PTX were further analyzed based on mathematical kinetics models. The zero-order and first-order release models[61,62] are described by the following equations, respectively

$$M_t = kt \tag{1}$$

$$\ln(1 - M_t/M_\infty) = -kt \tag{2}$$

Here, M_t means the cumulative release amount at time t, and M_∞ is the maximal amount of the released drug at infinite time. k means the zero-order or first-order rate constant expressed in percentage/time or time^{-1}, which is influenced by the chemical composition, geometric factors of the hydrogel matrix, and drug diffusivity from the hydrogel.

2.7. Cellular Experiments. *2.7.1. Cell Culture.* Human ovarian cancer cell line SKOV-3 was purchased from the Cell Bank of the Chinese Academy of Sciences (Shanghai, China). The cells were cultured in McCoy's 5A medium (Gibco) containing fetal bovine serum (FBS, 10%), penicillin (100 U/mL), and streptomycin (100 mg/mL) and incubated under a 5% CO_2 atmosphere at 37 °C.

2.7.2. Cellular Uptake of Micelles. The cellular uptake of PtGel conjugate micelles was investigated using coumarin-6 (Co-6) as a fluorescence probe, which was encapsulated into the hydrophobic cores of PtGel conjugate micelles. Briefly, Co-6 (15 mg) and PtGel conjugate (0.25 g) were dissolved in 3 mL of CH_2Cl_2 to form a uniform solution, and then the solvent was removed by rotary evaporation and lyophilization. Next, the polymer/Co-6 mixture was dissolved in McCoy's 5A medium, and the undissolved Co-6 was removed via centrifuge and filtration through a 0.22 μm filter to obtain a homogenous and sterilized solution. The exact amount of Co-6 loaded in the micelle solutions was determined by HPLC at a wavelength of 460 nm [mobile phase: acetonitrile/water (v/v) = 60/40].

SKOV-3 cells were seeded onto sterilized glass slides in 12-well plates at a density of 1.5 × 10^4 cell per well in the presence of 0.5 mL of medium and incubated at 37 °C for 24 h. The medium was then replaced with 1 mL of fresh culture medium containing Co-6-loaded PtGel conjugate (polymer concentration: 100 μM). After incubation at 37 °C for 0.5, 2, 6, and 24 h, the medium was extracted, and the cells were gently washed with PBS three times and fixed with 4 wt % paraformaldehyde solution for 15 min. The cell nuclei were stained with 4′,6-diamidino-2-phenylindole (DAPI, 0.1 wt % Triton X-100 solution in PBS). The cellular uptake of micelles was observed under a confocal laser scanning microscope (CLSM, C2$^+$, Nikon) through fluorescein isothiocyanate (FITC) and DAPI channels.

2.7.3. In Vitro Cytotoxicity Analysis. Cytotoxicity of the PtGel conjugate solution and its PTX-loaded solution was evaluated via the Cell Counting Kit-8 (CCK-8, Dojondo) assay. The samples were filtrated using 0.22 μm filters to obtain sterilized solutions before the experiment. SKOV-3 cells were cultured in 96-well plates at a density of 4 × 10^3 cell/well in the presence of 100 μL of culture medium and incubated at 37 °C for 12 h. Next, the medium was replaced with 200 μL of fresh medium containing PtGel conjugate, PTX-loaded PtGel conjugate, or PTX-loaded PLEL polymer at indicated concentrations (n = 6 for each group). After incubation at 37 °C for 48 h or 72 h, the cells were subjected to the CCK-8 assay, and the optical density at 450 nm was measured on a microplate reader (BioTek, ELx808). Cells without any polymer or drug treatment were regarded as the control group. The relative viability of treated cells was calculated as following

$$\text{viability (\%)} = \frac{\text{OD}_{\text{treat}} - \text{OD}_{\text{blank}}}{\text{OD}_{\text{control}} - \text{OD}_{\text{blank}}} \times 100\% \tag{3}$$

The in vitro synergistic cytotoxicity of PTX and PtGel conjugate was evaluated through the combination index (CI) analysis based on the Chou−Talalay method[63] by the following equation

$$\text{CI} = \frac{(D)_1}{(D_x)_1} + \frac{(D)_2}{(D_x)_2} \tag{4}$$

Here, $(D)_1$ and $(D)_2$ are the inhibitory concentrations (ICs) of drug 1 and drug 2 in the combination system at a given inhibitory rate. $(D_x)_1$ and $(D_x)_2$ represent the IC values of drug 1 and drug 2 when administrated alone, respectively. The IC values were determined by fitting the cell viability against the drug concentration on the logarithmic scale using SPSS software. A CI value <1 indicates a synergistic effect of the combination system, whereas CI values = 1 and >1 represent additive and antagonistic effects, respectively.

2.8. In Vivo Anticancer Experiments. *2.8.1. Xenograft Tumor Models on Nude Mice.* Female BALB/c nude mice, 5 weeks old, were purchased from the Shanghai Laboratory Animal Resource Center. Animals were raised under pathogen-free conditions. All experiments obeyed the "Principles of Laboratory Animal Care" (NIH publication #85-23, revised 1985) and were approved by the Ethics Committee of Fudan University. Ovarian cancer xenograft models were built using a two-step tissue block graft method. First, SKOV-3 cells (5 × 10^6 cells) in 100 μL of McCoy's 5A suspensions without FBS were injected subcutaneously under the first mammary gland of nude mice to develop tumors. When the tumor volume reached 600−800 mm^3, the animals were sacrificed, and tumors were dissected into small tissue fragments around 2 mm^3, while necrotic tissues were removed if there were any. The tissue blocks were then implanted into the same location of healthy nude mice by a trocar for new tumor growth.

2.8.2. Noninvasive Detection of Intratumoral Degradation of Fluorescence-Labeled PtGel. To noninvasively evaluate the in vivo maintenance of the PtGel system, a rhodamine B (RB)-conjugated PLEL triblock copolymer was introduced as a fluorescence probe. The RB−PLEL conjugate was synthesized via esterification between −COOH of RB and −OH on the hydrophobic end of the PLEL copolymer, as previously reported.[64] Briefly, the PLEL copolymer (2.04 g, 0.004 mol, synthesized as shown in Section 2.2.4 and dehydrated from azeotropic evaporation with toluene) was dissolved in CH_2Cl_2, and RB (0.48 g, 0.01 mol), DCC (0.42 g, 0.02 mol), and DMAP (0.24 g, 0.02 mol) were added into the system and stirred for 24 h in the dark under 25 °C. After the completion of the reaction, a few drops of water were added into the mixture to turn extra DCC into indissoluble DCU, which was then removed by filtration. The crude products were precipitated by ethyl ether and dialyzed against deionized water for 48 h to remove unreacted RB and then lyophilized to obtain the final products. The RB content in the conjugated polymer was determined by UV−vis detection at 560 nm. When the tumor volume of nude mice reached around 200 mm^3, 100 μL of PtGel conjugate solution (25 wt %) containing 1 wt % RB−PLEL copolymer was injected intratumorally. Observation was performed on an optical and X-ray small animal imaging system (In-Vivo Xtreme, Bruker).

2.8.3. In Vivo Anticancer Effect on Ovarian Tumor-Bearing Nude Mice. SKOV-3 ovarian tumor-bearing nude mice were divided randomly into six groups (n = 6) and treated with (A) saline (50 μL), (B) PtGel (50 μL, 32 mg/kg cisplatin), (C) PTX-loaded PLEL hydrogel (50 μL, 10 mg/kg PTX), (D) PTX-loaded PtGel (50 μL, 32 mg/kg cisplatin and 10 mg/kg PTX), (E) PTX-loaded PtGel (100 μL, 64 mg/kg cisplatin and 20 mg/kg PTX), and (F) free cisplatin/PTX

DOI: 10.1021/acsami.7b11998
ACS Appl. Mater. Interfaces 2017, 9, 40031−40046

solution (10.7 mg/kg cisplatin and 3.33 mg/kg PTX, three times). Treatment was performed when the tumor volume of nude mice reached around 100−150 mm^3. For groups A−E, saline and hydrogel solutions were administrated via intratumoral injection on day 1. Hydrogel formulations were prepared using the same method as the in vitro release experiment, with 25 wt % polymer concentration and 4 mg/mL PTX loaded and were filtrated using 0.22 μm filters before administration. For group F, free cisplatin and PTX in saline were injected intravenously via the tail vein three times on days 1, 10, and 19, with the total drug amount equal to the hydrogel formulation in group D. Specially, because PTX solution was diluted with saline from the commercial clinical PTX formulation containing Cremophor, an injection of dexamethasone (0.4 mg/kg) solution was administrated 0.5 h prior to PTX to prevent a possible allergic reaction caused by Cremophor.

The tumor size was measured twice per week and calculated using $V = a \times b^2/2$, where a and b were the longest and shortest diameters of the tumors. The body weight of mice was also measured as an indicator of systemic toxicity. On day 29 post treatment, the animals were sacrificed, and the tumors and organs were harvested, weighted, and treated with hematoxylin−eosin (H&E) staining for further examination. The micrographs of H&E staining were taken under an inverted fluorescence microscope (Axiovert 200, Zeiss).

2.9. Statistical Analysis. The significance of the differences between results was evaluated using the unpaired Student's t test. A p value <0.05 was considered statistically significant.

3. RESULTS

3.1. Synthesis and Characterization of the PtGel Conjugate. The synthesis pathway of the PtGel conjugate is illustrated in Scheme 1. Cisplatin was first oxidized into a Pt(IV) compound with two extra hydroxyl groups, and then the Pt(IV) compound was further reacted with succinic anhydride to acquire two carboxyl groups and obtain *cis,cis,trans*-$Pt(NH_3)_2Cl_2(OOCCH_2CH_2COOH)_2$. Meanwhile, the mPEG-PLGA diblock copolymer was synthesized via ring-opening polymerization of LA and GA using mPEG as the macroinitiator and $Sn(Oct)_2$ as the catalyst. Finally, the dicarboxyl Pt(IV) compound was used as the coupling agent to link two mPEG-PLGA copolymers, resulting in the formation of the Bi(mPEG-PLGA)−Pt(IV) (PtGel) conjugate.

Scheme 1. Synthesis Pathway of the Bi(mPEG-PLGA)−Pt(IV) (PtGel) Conjugate

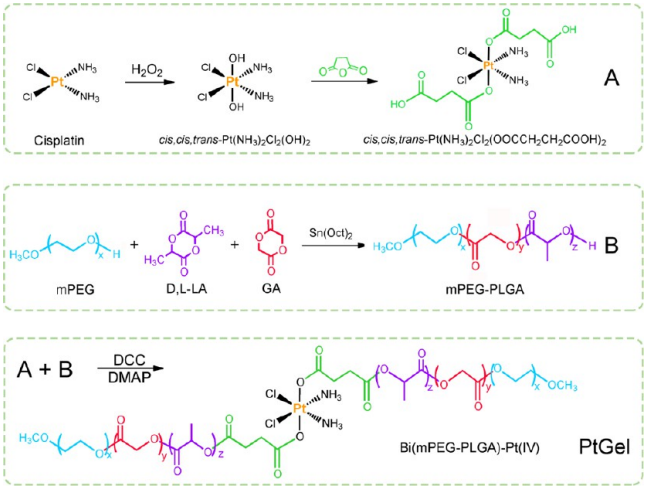

The molecular compositions of *cis,cis,trans*-$Pt(NH_3)_2Cl_2(OOCCH_2CH_2COOH)_2$, mPEG-PLGA copolymer, and PtGel conjugate were determined by ^{1}H NMR measurements. For the dicarboxyl Pt(IV) compound, the integral ratio of proton signals of $-COOH$, $-NH_3$, and $-CH_2CH_2COOH$ (12.07, 6.48, and 2.51 ppm, respectively) was approximately 1:3:2 (Figure 2a), indicating the successful synthesis of the desired product. For the mPEG-PLGA diblock copolymer, the number average MW (M_n) was calculated via the peak areas at 3.38 ppm ($-OCH_3$), 4.80 ppm ($-CH_2COO-$), and 5.20 ppm ($-CH(CH_3)COO-$) (Figure 2b), according to the previous publication.[56] As for the PtGel conjugate, not only the new proton peaks of $-NH_3$ and $-OOCCH_2CH_2COO-$ were observed at 5.97 and 2.66 ppm, respectively (Figure 2c) but also the mole ratio calculated from the peak areas of i ($-OCH_3$) and k ($-OOCCH_2CH_2COO-$) was approximately 3:4, which confirmed the success of the coupling reaction.

MWs and their distributions of all synthesized polymers were further determined by the GPC analysis, as shown in Figure 3. Similar to the conventional BAB-type PELE triblock copolymer that was synthesized using efficient HMDI as the coupling agent, the PtGel conjugate exhibited a unimodal distribution manner and an almost doubled MW of the original mPEG-PLGA. Meanwhile, the Pt content of the PtGel conjugate was also confirmed by ICP−OES measurements, and the value of 3.34 wt % was quite close to that of the theoretical calculation (3.38 wt %). All these results clearly demonstrated that the desired PtGel conjugate was successfully obtained. The molecular parameters of all copolymers synthesized in this study are listed in Table 1.

3.2. Sol−Gel Transition of Concentrated Polymer Aqueous Solutions. An appropriate sol−gel transition temperature is an important prerequisite for injectable thermosensitive hydrogels as drug-delivery carriers. Both mPEG-PLGA polymers and PtGel conjugates were soluble in water at an ambient temperature, and their concentrated aqueous solutions could spontaneously turn into semisolid gels upon heating. Under the same polymer concentration of 25 wt %, the PtGel conjugate/water system exhibited a lower sol−gel transition temperature (35 °C) compared with that of mPEG-PLGA (38 °C), as presented in Table 1. Also, different from the colorless mPEG-PLGA/water system, the PtGel conjugate solution presented a yellow color (inset images in Figure 4) because of the introduction of the Pt(IV) prodrug compound.

The storage modulus (G') and viscosity (η) of the mPEG-PLGA and PtGel aqueous solutions (25 wt %) as a function of temperature were further examined by dynamic rheological measurements, and the results are shown in Figures 4 and S1. At room or low temperature, both the polymer aqueous solutions exhibited a low modulus (<0.1 Pa), implying their good flowability. As the temperature went up, an abrupt increase of several orders of magnitude in G' and η occurred, indicating the formation of in situ physical hydrogels. The sol−gel transition temperature obtained from rheological measurements was well-consistent with that determined by the tube-inverting method, as displayed in Table 1. Meanwhile, the introduction of the Pt(IV) prodrug also brought a significant increase in the maximum of the modulus and viscosity of the PtGel conjugate/water system, reflecting a remarkable improvement of strength performance of the polymer−Pt(IV) conjugate hydrogel.

3.3. Preparation of Drug-Loaded Hydrogel Formulations. The PtGel conjugate/water system was tried for loading PTX, a very hydrophobic anticancer drug (solubility is approximately 4 μg/mL in water). Simple physical mixing of PTX with the conjugate aqueous solution could not achieve a

DOI: 10.1021/acsami.7b11998
ACS Appl. Mater. Interfaces 2017, 9, 40031−40046

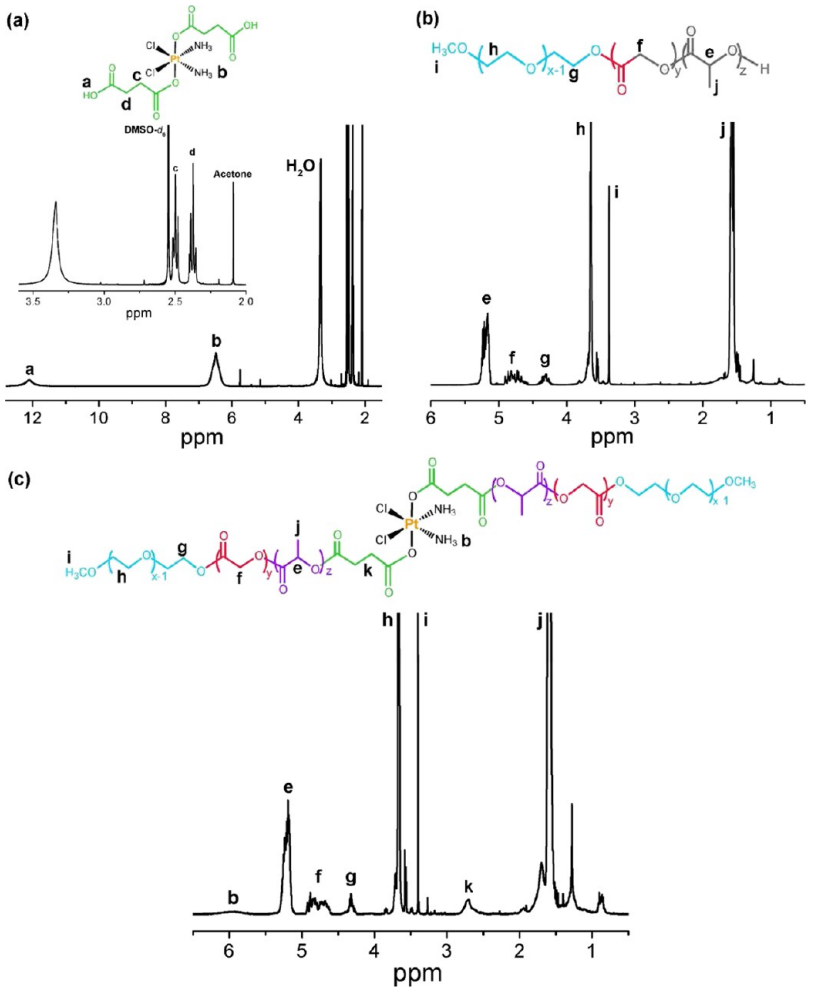

Figure 2. ^{1}H NMR spectra of (a) *cis,cis,trans*-$Pt(NH_3)_2Cl_2(OOCCH_2CH_2COOH)_2$ in DMSO-d_6, (b) mPEG-PLGA copolymer, and (c) PtGel conjugate in $CDCl_3$.

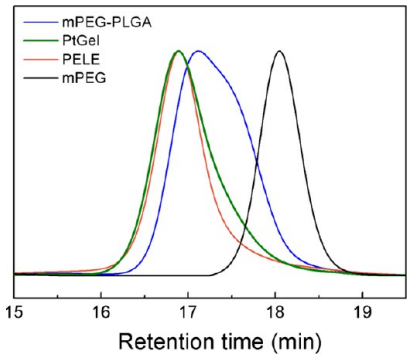

Figure 3. GPC chromatograms of mPEG (750), mPEG-PLGA, PELE polymers, and PtGel conjugate.

uniform formulation with a high drug-loading amount that we desired. Actually, when PTX concentration reached 4 mg/mL, continuous stirring of several days still obtained a turbid suspension.

Hence, we adopted a two-step method to prepare the PTX-loaded PtGel formulation: PTX and PtGel conjugate were first dissolved together in acetone; then, the solvent was removed by rotary evaporation, followed by lyophilization. After redissolving the mixture in water (polymer concentration: 25 wt %; PTX loading amount: 4 mg/mL), a uniform and steady solution with a transparent yellow color was obtained. Consequently, an enhancement of 1000-fold of PTX solubility was achieved in the 25 wt % PtGel conjugate solution. Also, there was almost no loss of drug during the whole preparation process, and the drug-loading efficiency or encapsulation efficiency was close to

Table 1. Parameters of Polymers Synthesized in This Study

sample	M_n [a]	M_n [b]	(M_w/M_n) [b]	LA/GA ratio [a]	sol−gel transition temperature [c] (°C)
mPEG-PLGA	750−1870	2530	1.34	6/1	38
Bi(mPEG-PLGA)−Pt(IV) (PtGel)	750−4260−750	4480	1.26	6/1	35
mPEG−PLGA−mPEG (PELE)	750−4060−750	4580	1.25	6/1	41
PLGA−PEG−PLGA (PLEL)	1780−1500−1780	3490	1.26	6/1	31

[a] M_ns of the mPEG block and PEG block were provided by Aldrich, and M_n of the PLGA block was calculated via ^{1}H NMR. [b] Measured by GPC. [c] Determined by the tube-inverting method. The polymer concentration was 25 wt %.

DOI: 10.1021/acsami.7b11998
ACS Appl. Mater. Interfaces 2017, 9, 40031−40046

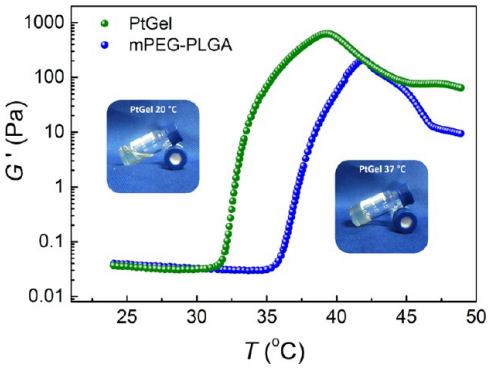

Figure 4. Storage modulus (G') of the aqueous solutions of the mPEG-PLGA polymer and PtGel conjugate as a function of temperature. Heating rate: 0.5 °C/min; oscillatory frequency: 10 rad/s; polymer concentration: 25 wt %. The inset photographs show the PtGel conjugate/water system (25 wt %) exhibiting sol and gel states at 20 and 37 °C, respectively.

100%. Finally, in this PTX-loaded PtGel formulation, the drug-loading concentration of Pt was equivalent to 12.87 mg/mL cisplatin, and the mole ratio of PTX and cisplatin reached 1:9.

Because the mPEG-PLGA and PELE aqueous solutions at the same concentration (25 wt %) exhibited higher sol−gel transition temperatures (38 and 41 °C, respectively) than the physiological temperature, making them unsuitable for in vivo biomedical applications, another triblock copolymer, which is an ABA-type PLGA-PEG-PLGA (PLEL) copolymer with a similar block length of PEG and PLGA and a similar LA/GA ratio (as presented in Table 1), was selected as a comparison system in the monodrug delivery of PTX.

We further studied the temperature-responsive gelation behavior of the PTX-loaded PtGel formulation. Its sol−gel transition temperature determined by the tube-inverting method was 33 °C, which was 2 °C lower than that of the PtGel conjugate solution without PTX at the same polymer concentration. The images in Figure 5a show the sol state at 20 °C and gel state at 37 °C of the PTX-loaded PtGel formulation. Meanwhile, the dynamic rheological test demonstrated that the incorporation of PTX into the PtGel system not only decreased its sol−gel transition temperature but also significantly increased its maximum of the modulus and viscosity (Figures 5a and S2a). By contrast, the loading of PTX into the PLEL solution had no obvious influence on the sol−gel transition temperature of the PLEL solution as well as its rheological properties, as presented in Figures 5b and S2b.

3.4. Micelle Behavior of the PtGel Conjugate Solution with or without PTX. To explore the possible interaction between PTX and the PtGel system, we studied and compared the micelle behaviors of the PtGel conjugate solution and PTX-loaded PtGel conjugate solution in the state of diluted solution. First, we confirmed the formation of micelles of the PtGel conjugate and PTX−PtGel conjugate mixture in water via DLS and TEM, as displayed in Figure 6a,b. The average D_h of PtGel conjugate micelles in water was 17 nm at the conjugate concentration of 1 wt % under 25 °C. The loading of PTX into the PtGel conjugate solution had no obvious effect on the formation of micelles. The size of micelles and size distribution were similar to that of pure PtGel conjugate micelles. We also measured the CMC of PtGel conjugate solutions with or without PTX using DPH as a hydrophobic dye probe. The results showed that both the CMC values were around 0.022 wt %, and no significant difference was observed between them, as presented in Figure 6c.

Interestingly, the observation of the micelle size with increasing temperature found that the PTX-loaded PtGel conjugate micelles exhibited an earlier trend of micellar aggregation than pure PtGel conjugate micelles, as shown in Figure 6d. This feature well-coincided with the results of rheological measurements (Figures 5a and S2a) and suggested that the incorporation of PTX increased the global hydrophobicity of the PtGel system, leading to a lower sol−gel transition temperature and a higher gel modulus.

3.5. In Vitro Drug Release. The in vitro release experiments were conducted under physiological conditions (37 °C, pH 7.4). As shown in Figure 7a, the release of Pt from the PtGel conjugate hydrogel exhibited a well-controlled manner and lasted for over 70 days. No burst release was

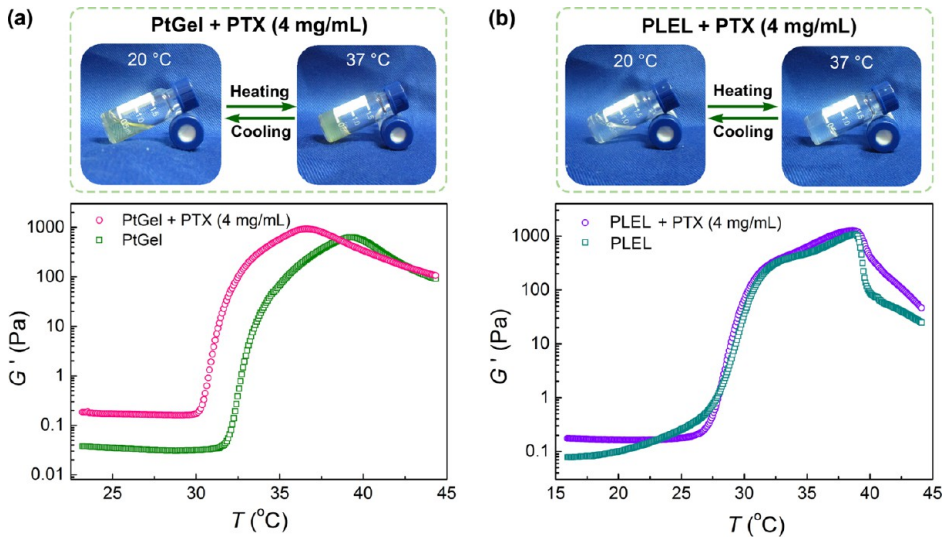

Figure 5. Properties of drug-loaded hydrogel formulations. Photographs of PTX-loaded (a) PtGel and (b) PLEL aqueous solutions exhibiting sol and gel states at 20 and 37 °C, respectively, and the storage modulus G' of the polymer solutions with or without PTX as a function of temperature. Heating rate: 0.5 °C/min; oscillatory frequency: 10 rad/s; PTX loading amount: 4 mg/mL; polymer concentration: 25 wt %.

DOI: 10.1021/acsami.7b11998
ACS Appl. Mater. Interfaces 2017, 9, 40031−40046

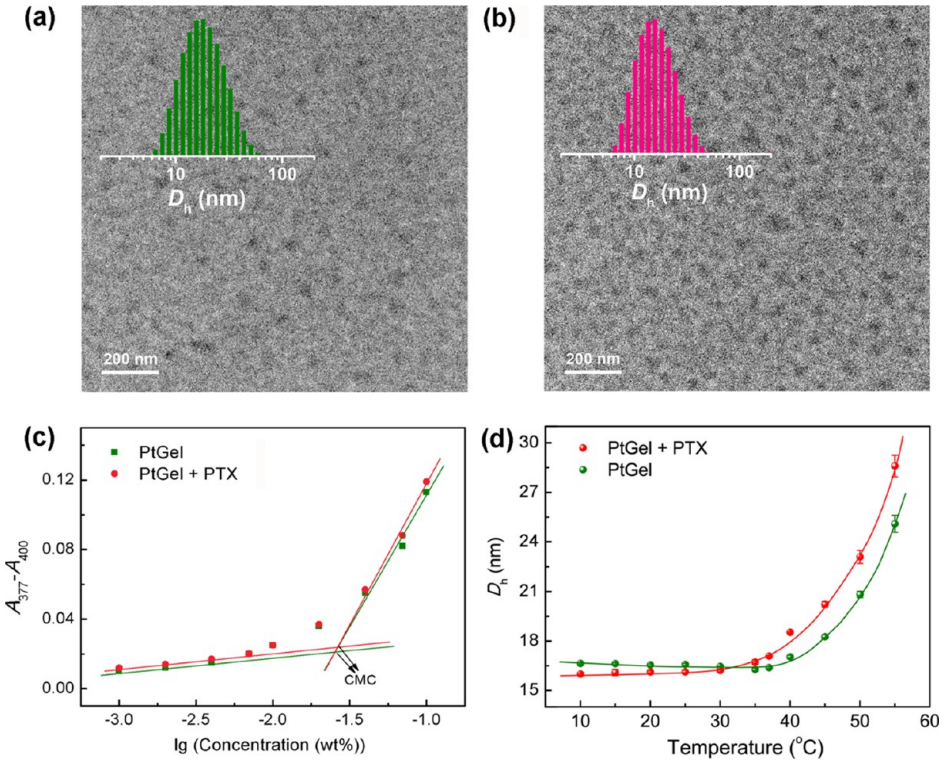

Figure 6. Micelle behaviors of the PtGel conjugate solutions with or without PTX. (a,b) TEM images of micelles in the PtGel conjugate aqueous solution and PTX-loaded PtGel conjugate solution, respectively. The inset images show the corresponding distribution of the micelle size (intensity-average) measured by DLS. (c) CMC determination of the PtGel conjugate solution and its PTX-loaded solution by extrapolation of the difference of absorbance at 377 and 400 nm. The measurements were carried out at 20 °C. (d) *Z*-average micelle size in the PtGel conjugate solution and PTX-loaded PtGel conjugate solution as a function of temperature. Polymer concentration: 1 wt %; PTX loading amount: 0.16 mg/mL.

observed at the initial stage, and the cumulative release amount was over 85% at the later stage. Meanwhile, the loading of PTX into the PtGel conjugate hydrogel had no significant influence on the release profile of Pt from the hydrogel matrix.

Because of the incorporation of PTX into the hydrophobic cores of PtGel conjugate micelles, PTX might be released in the form of PtGel conjugate micelles containing PTX or their micellar aggregates. To avoid the possible mass loss caused by filtration before the HPLC measurement, the release medium collected was first lyophilized and then redissolved in acetonitrile to ensure that the total amount of released PTX could be fully detected. As shown in Figure 7b, PTX released from both the PtGel and PLEL hydrogels exhibited a similar release curve in the first 12 days. After that, an abruptly accelerated release of PTX from the PLEL hydrogel was observed, and nearly 40% of the loaded drug was released in the next 2 weeks. Meanwhile, the hydrogel matrix itself gradually swelled and grew into a loose, vulnerable structure and broke up into floccules eventually because of the degradation of the hydrogel via the hydrolysis of PLGA segments.[43,49] It is obvious that the accelerated release of PTX from the PLEL hydrogel was attributed to the degradation and the subsequent structure change of the hydrogel matrix.

In sharp contrast, PTX loaded in the PtGel system was released in an almost constant rate, and a total release amount of 75% was achieved within 75 days. Meanwhile, the integrity of the PtGel conjugate hydrogel matrix was maintained up to 40 days merely accompanying with shrinking in volume, and then the gel broke into several pieces at the last stage, even if the PtGel system underwent the hydrolysis of PLGA segments throughout the whole release period. The different release profiles of PTX from the two hydrogels were mainly because of their different gel strengths and stabilities. In addition, the loading of PTX into the PtGel matrix further improved its strength and stability, as demonstrated via the rheological study in Figure 5. These findings indicate that the PtGel system is an ideal system for the sustained delivery of PTX.

Taking them altogether, as illustrated in Figure 7c, the release of Pt and PTX from the PTX-loaded PtGel system exhibited a sustained codelivery manner as long as 75 days, and the cumulative release amounts of the two drugs exceeded 75%. The release data were further evaluated via mathematical models of the release kinetics. The results showed that the release of Pt from the PtGel system was well-fitted by the first-order release equation, whereas the PTX release from the PtGel system was in good consistence with the zero-order kinetics, both with good correlation coefficients ($R^2 \approx 0.99$). The fitting parameters are summarized in Table 2.

3.6. Cellular Uptake, In Vitro Cytotoxicity, and Synergistic Effect. Cellular uptake of the PtGel conjugate micelles was observed using SKOV-3 cells under a CLSM. The PtGel conjugate concentration used in the cellular uptake experiment was fixed at 100 μM. Co-6, a fluorescence label, was entrapped into the hydrophobic cores of PtGel conjugate micelles, and the concentration of loaded Co-6 was determined by HPLC to be 24.6 μg/mL. The cell nuclei were stained with DAPI (blue) to locate the cells.

As shown in Figure 8, after incubation of 0.5 h, intense green fluorescence of Co-6 had spread over the cytoplasm, indicating that the PtGel conjugate micelles successfully and efficiently entered into the cells via endocytosis. As the incubation time increased to 2 h, the intensity of green fluorescence in cells

DOI: 10.1021/acsami.7b11998
ACS Appl. Mater. Interfaces 2017, 9, 40031−40046

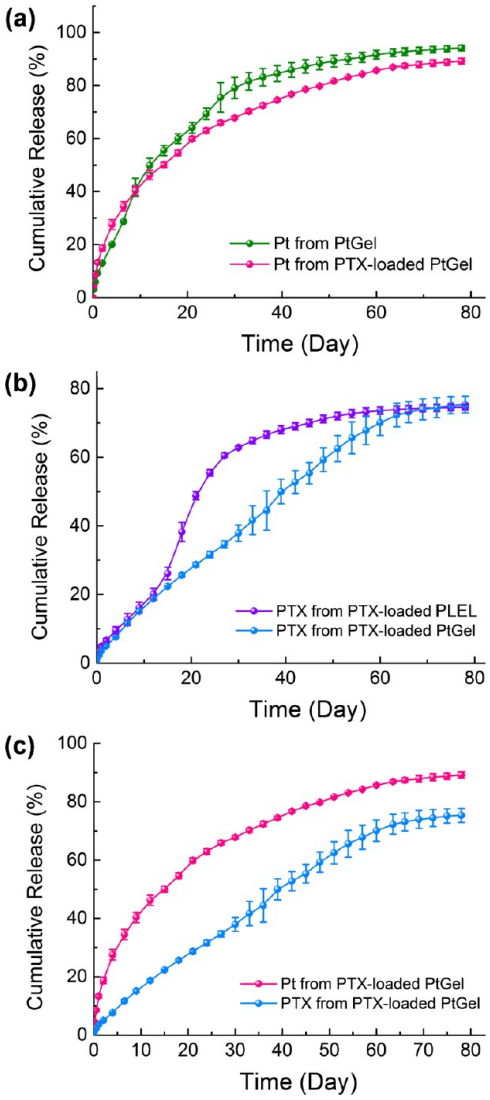

Figure 7. In vitro release profiles of (a) Pt from the PtGel system and PTX-loaded PtGel system; (b) PTX from the PTX-loaded PtGel system and PTX-loaded PLEL hydrogel; and (c) Pt and PTX from the PTX-loaded PtGel system. Polymer concentrations: 25 wt %; PTX loading amount: 4 mg/mL.

Table 2. Mathematical Kinetics Assessments of the In Vitro Release Data

first-order release	k	M_∞	R^2
Pt from PtGel	0.061	93.6	0.990
Pt from PTX-loaded PtGel	0.050	89.2	0.992
zero-order release	k		R^2
PTX from PTX-loaded PtGel	1.446		0.990

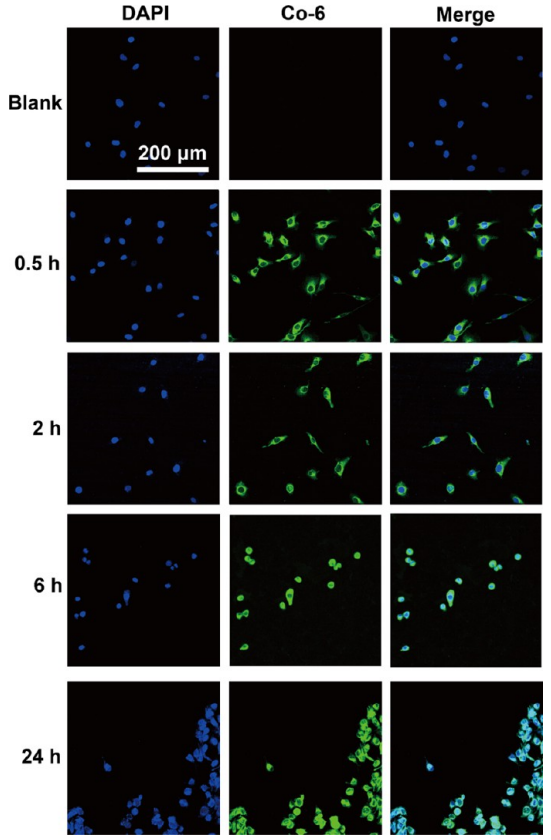

Figure 8. Cellular uptake of the Co-6-labeled PtGel conjugate micelles in SKOV-3 cells after incubation for 0.5, 2, 6, and 24 h. CLSM images taken from the DAPI channel (column 1, blue) and FITC channel (column 2, green) and merged images of both channels (column 3). The first row shows the cells incubated with the PtGel conjugate solution without Co-6 as the blank control.

further increased, and the green fluorescence was observed in the cell nuclei. Further increasing the incubation time to 6 and 24 h, more intense green fluorescence was observed in the cell nuclei, as shown in the merge column. Meanwhile, the morphology of the cells started to change from a spindle shape to spherical shape. This feature also confirmed that the PtGel conjugate micelles have the ability to enter the cell nuclei, be reverted to cisplatin upon intracellular reduction, and then bind with DNA to induce cell apoptosis.[53,54]

The in vitro cytotoxicity of the PTX-loaded PtGel conjugate solution was evaluated quantitatively via the CCK-8 assay using SKOV-3 cells. The pure PtGel conjugate solution and PTX-loaded PLEL copolymer solution were selected as the monodrug controls. As shown in Figure 9a–c, the cytotoxicity of all three systems exhibited a positive correlation with the concentration or time. When the PtGel conjugate solution was administrated alone, its IC_{50} values at 48 and 72 h were 208.4 and 128.6 μM, respectively, indicating that a higher inhibition rate was achieved as the treatment time prolonged. For the cells treated with the PTX-loaded PLEL copolymer solution, its IC_{50} values at 48 and 72 h were 0.0082 and 0.0081 μM, respectively, which had no obvious time dependence and were at a much lower level than that of the PtGel conjugate solution. When PTX and PtGel conjugates were administrated together in the dual-drug-delivery system, their IC_{50} values at 48 and 72 h dropped to 0.0573 μM (Pt)/0.0073 μM (PTX) and 0.0556 μM (Pt)/0.0071 μM (PTX), respectively.

To quantitatively evaluate the synergistic effect of this PTX–PtGel combination, we calculated the CI based on the Chou–Talalay method. As shown in Figure 9d, after 48 or 72 h of treatment, the CI values were lower than 1 in most inhibition conditions, indicating a synergistic effect of this PTX–PtGel micelle system. Interestingly, the correlations between the CI values and inhibition rate after 48 and 72 h of treatment were totally different: one was positive, and the other was negative. This finding indicated that the treatment duration also has a

DOI: 10.1021/acsami.7b11998
ACS Appl. Mater. Interfaces 2017, 9, 40031–40046

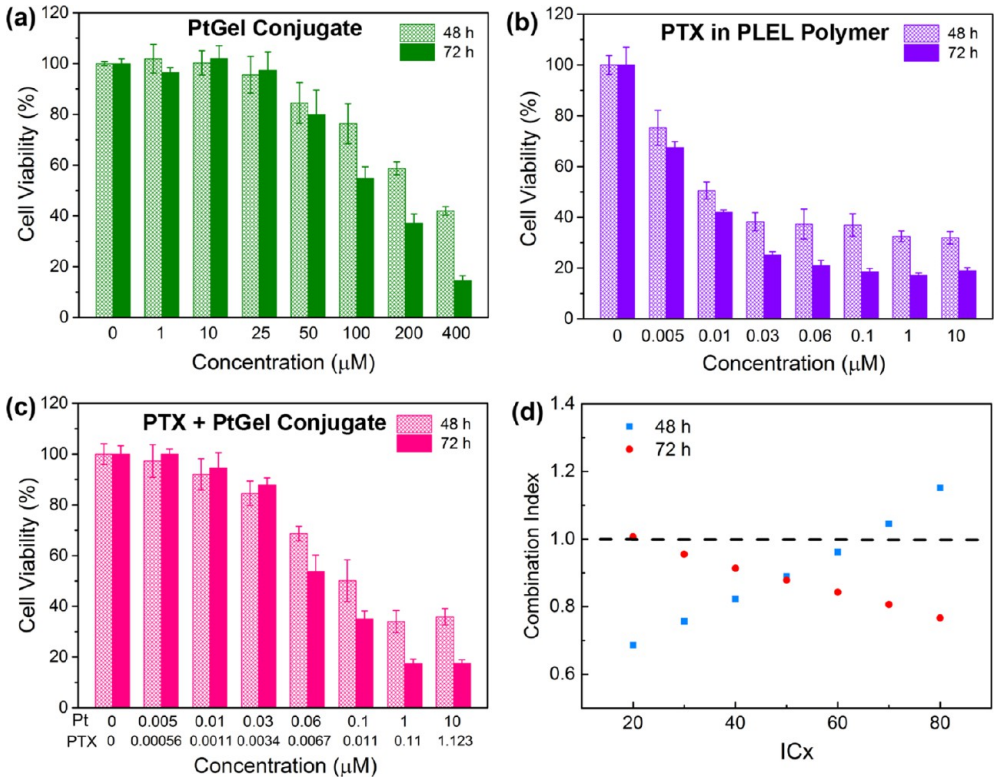

Figure 9. In vitro cytotoxicity of the PtGel conjugate solution (a), PTX-loaded PLEL copolymer solution (b), and PTX-loaded PtGel conjugate solution (c) as a function of the drug concentration after incubation of 48 and 72 h. The blank control with culture medium only was set as 100% cell viability. Each point represents the mean ± SD; n = 6. (d) CI vs IC_X after 48 and 72 h of treatment of the PTX−PtGel conjugate combination system.

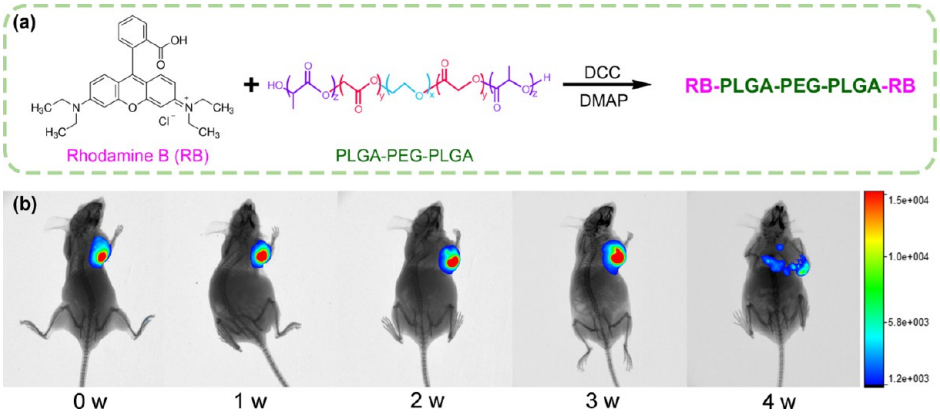

Figure 10. Fluorescent imaging to monitor the in vivo degradation of the PtGel conjugate hydrogel. (a) Synthetic pathway of the rhodamine B-conjugated PLGA−PEG−PLGA copolymer (RB−PLEL) as a fluorescence probe of hydrogel. (b) Merge photographs of X-ray and fluorescent images of the RhB-labeled PtGel system in tumor-bearing nude mice. The PtGel conjugate concentration was 25 wt %, and the PtGel conjugate hydrogel contained 1 wt % RB−PLEL polymers.

significant influence on the synergistic effect of this dual-drug-delivery system.

3.7. In Vivo Animal Experiments. A SKOV-3 ovarian cancer xenograft model in nude mice was constructed for the in vivo study. We first monitored the in vivo degradation of the PtGel conjugate hydrogel in a real-time and noninvasive manner by introducing a RB-conjugated PLEL copolymer into the PtGel system. The RB-conjugated PLEL copolymers were synthesized by covalently attaching RB molecules to the two hydrophobic ends of PLEL copolymers, as described in Figure 10a. The resultant RB−PLEL copolymer was soluble in water, and its RB content determined by UV spectrometer was 3.56 wt %. The incorporation of 1 wt % RB−PLEL polymers into the PtGel system produced a stable and strong red fluorescence and had no obvious influence on the temperature-induced gelation properties of the PtGel system. Therefore, this RB−PLEL copolymer could act as a probe for the noninvasive detection of the in vivo degradation of the PtGel system.

After the intratumoral injection of 100 μL of the RB-labeled PtGel conjugate hydrogel, an obvious red fluorescence was observed in the tumor under Xtreme, as shown in Figure 10b. As the time went by, the fluorescence intensity first increased and then decayed, and the fluorescence signal gradually spread to a broader area surrounding the tumor. The fluorescence

DOI: 10.1021/acsami.7b11998
ACS Appl. Mater. Interfaces 2017, 9, 40031−40046

stayed visible for more than 4 weeks before totally fading away, indicating that the hydrogel could maintain its integrity in vivo for up to 1 month.

We further evaluated the in vivo anticancer efficacy of the PTX−PtGel dual-drug hydrogel delivery system on the nude mice model bearing ovarian tumor. Figure 11a presents the change in the tumor volume as a function of time after different treatments. In the saline group, the mice did not receive any treatment, and thus their tumor volumes rapidly increased over time. After a single administration of monodrug hydrogel formulations (PtGel or PTX−PLEL hydrogel), the growth of the tumor was efficiently inhibited in the first 2 or 3 weeks, yet an accelerated tumor growth was observed in the following stage. The combination treatment of PTX and PtGel (both 50 and 100 μL groups) achieved an excellent tumor inhibition effect after a single injection. In the group of PTX−PtGel (50 μL), the growth of tumor was almost completely suppressed in the initial 3 weeks, and then the tumor volume slowly started to rebound in the fourth week, which was attributed to the absence of sufficient drug dosage after the 3-week sustained dual-drug release. In the case of the high-dosage PTX−PtGel group (100 μL), the tumor volume of mice even started to shrink in the fourth week because of the continuous liberation of the dual-drug with effective dosage during the whole period of examination. For the mice receiving the multiple intravenous injections of free PTX and cisplatin combination, the tumor-inhibition efficacy was similar to the two monodrug hydrogel systems.

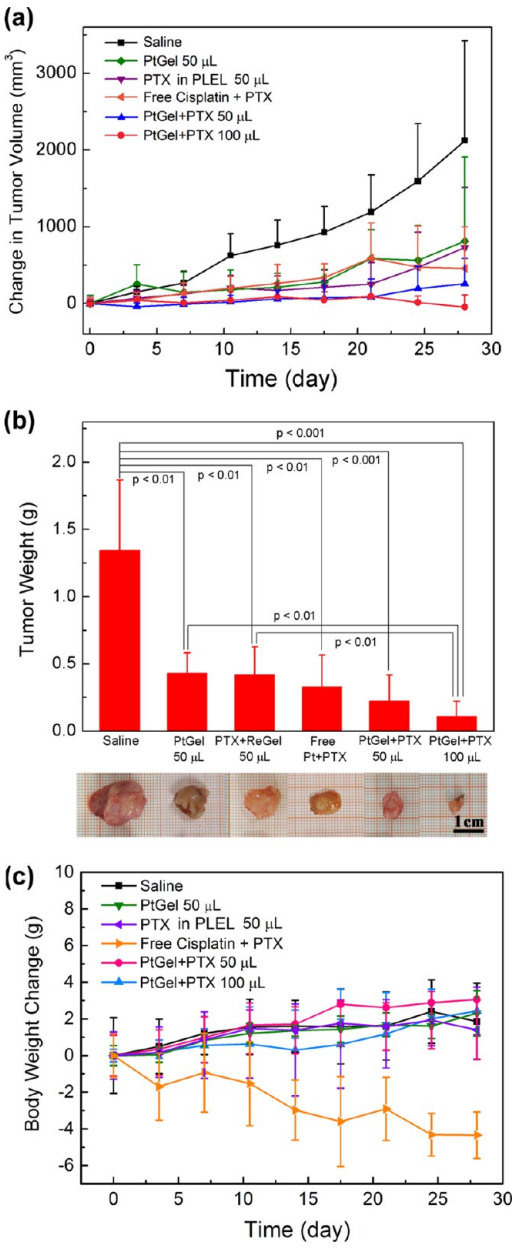

Figure 11. In vivo anticancer activity. Tumor volume changes (a), final mean tumor weights (b), and body weight changes (c) of mice receiving the indicated treatments. Each point represents the mean ± SD; n = 6. Photographs of tumors after dissection were taken on the 28th day post treatment.

Four weeks later, all animals were sacrificed, and tumors were excised and weighed. As shown in Figure 11b, the final average tumor weights of different groups were consistent with the variation trend of the tumor volume. There were significant statistical differences between the four drug-treated hydrogel groups and the saline group, as well as between the PTX−PtGel 100 μL group and the two monodrug hydrogel groups.

During the same period, we also recorded the change in the body weight of the animals over time as an indicator of the systematic toxicity of different treatment systems. As shown in Figure 11c, the body weight of mice receiving the treatment of free cisplatin and PTX combination exhibited a continuous descending trend, and the average decrease of the body weight reached 20% after treatment for 4 weeks. Two among the six mice died after the third intravenous injection. These results indicated that there were severe systematic side effects after intravenous injection of the combination of free cisplatin and PTX. For the two monodrug treated hydrogel groups and the untreated group, the body weight of mice increased in the first 2 weeks, but stopped increasing and even dropped at the later stage. This feature was attributed to an accelerated tumor growth at this stage, resulting in the suppression of the body weight. By contrast, the body weight of mice receiving the treatment of dual-drug hydrogel formulation at the low dosage (PTX−PtGel 50 μL) continuously increased during the whole experiment period. For the high-dosage group (PTX−PtGel 100 μL), the increase of the body weight of mice was slow in the initial 2 weeks, followed up presenting acceleration. The final average body weight of mice was very close to that of the low dosage group at 4 weeks post treatment.

After sacrifice of mice, various organs including heart, liver, spleen, lung, and kidney were isolated, and histological observation was performed to evaluate the systemic side effects after different treatments. The results shown in Figure 12 confirmed that all organ tissues of mice treated with different hydrogel formulations exhibited clear inherent structural profiles, and no obvious tissue abnormality or damage was observed. This indicated that the administration of different drug-loaded hydrogel formulations did not bring any significant systemic toxicity. By contrast, in the mice treated with free PTX and cisplatin combination, nephrotoxicity as evidenced by the damaged and exfoliated renal epithelial cells was clearly observed.

In addition, histological observation of tumor tissues was also carried out to check the efficacy of different treatment systems. In the saline group, cells in tumor tissues were tightly packed within the stroma, and necrosis or apoptotic cells were rarely observed. By contrast, for the animals receiving the treatment

DOI: 10.1021/acsami.7b11998
ACS Appl. Mater. Interfaces 2017, 9, 40031−40046

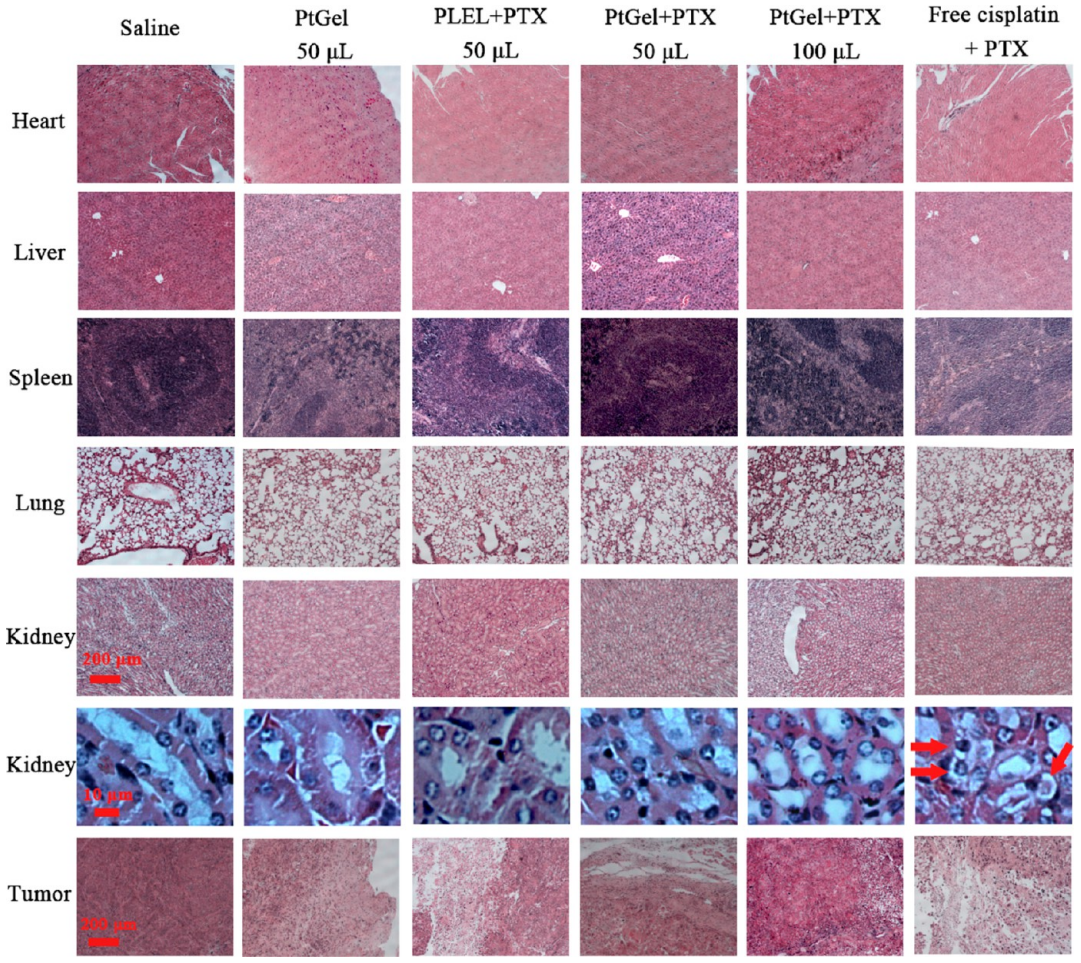

Figure 12. Representative histological microphotographs of heart, liver, spleen, lung, kidney, and tumor tissue of nude mice treated with saline, PtGel (50 μL), PTX in PLEL (50 μL), PTX + PtGel (50 μL), PTX + PtGel (100 μL), and free cisplatin + PTX, respectively. Red arrows show representative damaged and exfoliated renal tubular epithelial cells.

of PtGel, PTX, or their combination, different levels of tissue necrosis were found in their tumor tissues, including extensive shrinkage, fragmentation and absence of nuclei, widening of the interstitial space, and relative abundance of cytoplasm. All these features provided further evidence of the good anticancer efficacy and low systemic toxicity of our localized hydrogel delivery systems, especially dual-drug-delivery system.

4. DISCUSSION

The combination of free cisplatin and PTX has become a preferred chemotherapy option for various cancers, including ovarian cancer.[6,7] Therefore, it is of great significance to develop a combination delivery system of cisplatin and PTX that can realize the spatial−temporal synchronization of drug exposure, synergistic anticancer effects, and enhanced therapeutic potency. However, it is still very challenging to codeliver the two drugs in one vehicle because of their distinct chemical and physical properties.

In this study, we developed a strategy to realize the localized, sustained codelivery of cisplatin and PTX based on an injectable prodrug hydrogel. First, a thermosensitive PtGel conjugate was designed and synthesized via covalently linking a dicarboxyl Pt(IV) prodrug with mPEG-PLGA diblock copolymers with a stoichiometric ratio of 1:2. Compared with the original mPEG-PLGA diblock copolymer, the Pt(IV)-conjugated copolymer maintained the temperature-responsive gelling behavior, but exhibited a reduced sol−gel transition temperature and an increased gel strength owing to the increase of total hydrophobicity via the covalent introduction of the Pt(IV) prodrug (Figure 4). Compared with the HMDI-conjugated PELE hydrogel, the introduction of a very hydrophobic Pt(IV) prodrug also brought a lower sol−gel transition temperature for the PtGel system. These changes made the PtGel system more suitable as an injectable in situ gelation carrier for long-term codelivery of other drugs.

As is well-known, hydrophobic drugs can be incorporated into the hydrophobic cores of micelles made up of amphiphilic PEG/polyester block copolymers, which results in a dramatic increase of their solubility in the corresponding aqueous systems.[41,62] Herein, the amphiphilic Pt(IV)-containing conjugates also greatly solubilized the famous, hydrophobic anticancer drug PTX (1000-fold enhancement of solubility) because of the formation of micelles of PtGel conjugates in water. Meanwhile, we found that the loading of PTX into the PtGel conjugate/water system lowered its sol−gel transition temperature (from 35 °C decreased to 33 °C), but increased its gel strength (Figure 5). By contrast, no obvious influence was observed in the PTX-loaded PLEL hydrogel system without the Pt(IV) prodrug.

One hierarchy mechanism of physical gelation of PEG/PLGA copolymers has been suggested in our previous study.[41,56,65] In brief, amphiphilic block copolymers self-

DOI: 10.1021/acsami.7b11998
ACS Appl. Mater. Interfaces 2017, 9, 40031−40046

assemble into micelles with core−corona structures at a low or room temperature. As the temperature increases, the micelles further aggregate into a percolated micelle network because of the hydrophobic interaction between micelles, leading to the sol−gel transition on a macroscopic scale. Therefore, we also analyzed the micelle behavior of PtGel conjugate/water systems with or without PTX via DLS, TEM, and CMC measurements, as displayed in Figure 6. The results revealed that the incorporation of PTX had no obvious influence on the micelle formation and the CMC of PtGel conjugates in water, but it increased the capacity of micellar aggregation at a lower temperature. This finding suggested that the global hydrophobicity of the PtGel system was enhanced by the incorporation of PTX, which was responsible for the decrease in the sol−gel temperature and the increase in the gel strength.

In vitro release of both the dual-drug-loaded PtGel system and monodrug-loaded hydrogel systems was examined and compared (Figure 7). Unlike simple physical encapsulation of cisplatin into hydrogel matrices, which led to the rapid release of the drug,[44,50,51] the covalent conjugation of the Pt(IV) prodrug onto thermosensitive polymers greatly prolonged the release period of Pt. The incorporation of PTX into the PtGel conjugate hydrogel had no obvious influence on the release profile of Pt. Meanwhile, such an incorporation led to the enhanced gel strength and good persistence of integrity of the PtGel matrix (Figure 5), enabling the release of PTX in an almost constant release rate during the whole examined period. As a result, the PTX-loaded PtGel system realized a sustained release manner of the two drugs for as long as 2.5 months, and such a long-acting combined delivery of the two drugs has never been reported before, to the best of our knowledge. This feature also indicated that the thermosensitive PtGel system is suitable as a codelivery platform for cisplatin and other various anticancer drugs.

The cellular uptake of PtGel conjugate micelles was detected using Co-6 as the fluorescent indicator. CLSM imaging showed that the Co-6 labeled micelles could effectively enter the SKOV-3 cells, and a prolonged incubation time led to an increase of the fluorescence intensity both in the cytoplasm and nuclei of cells (Figure 8). This finding confirmed the effective uptake of PtGel conjugate micelles by cancer cells via endocytosis. It is worth pointing out that a quantitative measurement of the cellular uptake is required in the future work, which will be able to provide more detailed information on the cellular uptake of PtGel conjugate micelles.

In vitro cytotoxicity of the PtGel conjugates, PTX, and their combination system against SKOV-3 cancer cells was also confirmed, and the subsequent CI analysis showed that the combination drug-delivery system had an inspiring synergistic effect (Figure 9). Under different treatment durations (48 and 72 h), the correlation between the CI value and inhibition rate exhibited an opposite manner. We speculated that this phenomenon might be attributed to the influence of cisplatin treatment on the cell cycle. As reported by Vanhoefer et al.,[20] after treating with cisplatin for 24 h, the majority of cells was found in the S phase, and 48 h later, most of the cells just entered the PTX-sensitive G_2/M phase; this indicated a delay of cell−cycle transition caused by the treatment of cisplatin compared with normal cancer cells. Therefore, within a short incubation period for the PTX−cisplatin combination system, the efficacy of PTX was retarded to some extent, leading to an additive or even antagonist effect. Such a mechanism caused an increasing CI value as the PtGel conjugate concentration (also inhibition rate) increased after 48 h of treatment in the present study. After another 24 h of incubation, the delay of cell cycle transition induced by cisplatin and its corresponding influence on the PTX efficacy had come to an end, and hence a desired synergistic effect occurred as expected. These findings also provide beneficial guidance in the clinical application of the PTX−cisplatin combination therapy.

An RB-conjugated PLEL copolymer was synthesized and used as a fluorescence probe to noninvasively monitor the in vivo degradation of the PtGel conjugate hydrogel. Because the fluorescence strength detected by Xtreme is related to the detection distance and tissue thickness, it can be deduced that the increase of the fluorescence strength in the first several weeks was due to the diffusion of the polymers or their degradation products to the surrounding subcutaneous tissue. The noninvasive detection affirmed that the in vivo maintenance of the PtGel system lasted for up to 1 month, which was shorter than the in vitro persistence of the PtGel system, as presented in the in vitro drug-release experiment (Figure 7). This feature might be attributed to the complicated biological environment and low intratumoral pH that accelerated the hydrolysis of ester bonds of PLGA chains, which promoted the in vivo hydrogel degradation.

Finally, the in vivo anticancer effect of the codelivery drug system was evaluated on ovarian tumor-bearing nude mice. As shown in Figure 11a, the two groups of dual-drug hydrogel formulations with different dosages achieved much better anticancer efficacy than both the monodrug hydrogel groups and the free dual-drug solution group. It can be concluded that the unfavorable efficacy of systematic administration via intravenous injection was mainly due to the drug's low accumulation in the tumor and fast clearance from the blood stream. These features also led to severe systemic side effects, as reflected in the continuous decrease in the body weight, as shown in Figure 11c. Inspiringly, such a trend did not occur in any of the hydrogel-treated groups. In particular, the group treated with 100 μL of PTX−PtGel system exhibited the best overall condition. The tumor even started to shrink at 3 weeks postadministration, and the body weight kept growing continuously. The histological observation was also well in accordance with the above conclusions (Figure 12). Consequently, this PTX-loaded PtGel system has great potential as a codelivery drug system with increased anticancer effect while significantly lowering systematic side effects. In addition, it is worth noting that the ratio of PTX and the Pt drug has a significant effect on their synergistic anticancer efficacy, but it is not easy to widely tune the two drug ratios in the present system.

5. CONCLUSIONS

Herein, we developed a combination delivery system of hydrophilic cisplatin and hydrophobic PTX using an injectable Pt(IV)-conjugated copolymer hydrogel as the carrier and successfully realized a sustained codelivery of the two drugs with significantly different physical properties. A thermosensitive PtGel conjugate was synthesized by coupling mPEG-PLGA diblock copolymers with a Pt(IV) prodrug compound. The hydrophobic PTX could be effectively solubilized into the cores of micelles formed by the amphiphilic conjugates in water, and the concentrated conjugate solution containing PTX exhibited a sol−gel transition with increasing temperature. Both Pt and PTX were released from the dual-drug hydrogel formulation in a well-controlled sustained manner for 2.5 months. In vitro

DOI: 10.1021/acsami.7b11998
ACS Appl. Mater. Interfaces 2017, 9, 40031−40046

cytotoxicity experiments confirmed a synergistic anticancer effect of this dual-drug-delivery system against cancer cells. Finally, after a single intratumoral injection of this dual-drug hydrogel formulation into nude mice bearing human ovarian tumor, excellent in vivo anticancer efficacy and significantly reduced side effects were observed. In particular, the treatment of the dual-drug-delivery system with high dosage even caused the tumors to shrink at the later stage. Consequently, this PTX-loaded PtGel system not only shows great potential as a localized codelivery system of clinically used anticancer drugs cisplatin and PTX but also provides an important platform for long-term delivery of therapeutic agents with different water solubilities.

■ ASSOCIATED CONTENT

Supporting Information

The Supporting Information is available free of charge on the ACS Publications website at DOI: 10.1021/acsami.7b11998.

Rheological studies of the polymer aqueous solutions with or without drugs (PDF)

■ AUTHOR INFORMATION

Corresponding Author

*E-mail: yu_lin@fudan.edu.cn.

ORCID

Lin Yu: 0000-0001-7660-3367

Jiandong Ding: 0000-0001-7527-5760

Notes

The authors declare no competing financial interest.

■ ACKNOWLEDGMENTS

The work was supported by the National Natural Science Foundation of China (grant nos. 51273217 and 21474019), the State Key Project of Research and Development (grant no. 2016YFC1100300), and the Science and Technology Developing Foundation of Shanghai (grant no. 15JC1490300).

■ REFERENCES

(1) Jhaveri, A.; Deshpande, P.; Torchilin, V. Stimuli-Sensitive Nanopreparations for Combination Cancer Therapy. *J. Controlled Release* **2014**, *190*, 352−370.

(2) Lehár, J.; Krueger, A. S.; Avery, W.; Heilbut, A. M.; Johansen, L. M.; Price, E. R.; Rickles, R. J.; Short, G. F., 3rd; Staunton, J. E.; Jin, X.; Lee, M. S.; Zimmermann, G. R.; Borisy, A. A. Synergistic Drug Combinations Tend to Improve Therapeutically Relevant Selectivity. *Nat. Biotechnol.* **2009**, *27*, 659−666.

(3) He, C.; Tang, Z.; Tian, H.; Chen, X. Co-Delivery of Chemotherapeutics and Proteins for Synergistic Therapy. *Adv. Drug Delivery Rev.* **2016**, *98*, 64−76.

(4) Xiao, H.; Qi, R.; Li, T.; Awuah, S. G.; Zheng, Y.; Wei, W.; Kang, X.; Song, H.; Wang, Y.; Yu, Y.; Bird, M. A.; Jing, X.; Yaffe, M. B.; Birrer, M. J.; Ghoroghchian, P. P. Maximizing Synergistic Activity When Combining Rnai and Platinum-Based Anticancer Agents. *J. Am. Chem. Soc.* **2017**, *139*, 3033−3044.

(5) Greco, F.; Vicent, M. J. Combination Therapy: Opportunities and Challenges for Polymer−Drug Conjugates as Anticancer Nanomedicines. *Adv. Drug Delivery Rev.* **2009**, *61*, 1203−1213.

(6) Armstrong, D. K.; Bundy, B.; Wenzel, L.; Huang, H. Q.; Baergen, R.; Lele, S.; Copeland, L. J.; Walker, J. L.; Burger, R. A. Intraperitoneal Cisplatin and Paclitaxel in Ovarian Cancer. *N. Engl. J. Med.* **2006**, *354*, 34−43.

(7) Levasseur, L. M.; Greco, W. R.; Rustum, Y. M.; Slocum, H. K. Combined Action of Paclitaxel and Cisplatin against Wildtype and Resistant Human Ovarian Carcinoma Cells. *Cancer Chemother. Pharmacol.* **1997**, *40*, 495−505.

(8) Gilmore, K. A.; Lampley, M. W.; Boyer, C.; Harth, E. Matrices for Combined Delivery of Proteins and Synthetic Molecules. *Adv. Drug Delivery Rev.* **2016**, *98*, 77−85.

(9) Stathopoulos, G. P.; Antoniou, D.; Dimitroulis, J.; Michalopoulou, P.; Bastas, A.; Marosis, K.; Stathopoulos, J.; Provata, A.; Yiamboudakis, P.; Veldekis, D.; Lolis, N.; Georgatou, N.; Toubis, M.; Pappas, C.; Tsoukalas, G. Liposomal Cisplatin Combined with Paclitaxel Versus Cisplatin and Paclitaxel in Non-Small-Cell Lung Cancer: A Randomized Phase Iii Multicenter Trial. *Ann. Oncol.* **2010**, *21*, 2227−2232.

(10) Moore, K. N.; Herzog, T. J.; Lewin, S.; Giuntoli, R. L.; Armstrong, D. K.; Rocconi, R. P.; Spannuth, W. A.; Gold, M. A. A Comparison of Cisplatin/Paclitaxel and Carboplatin/Paclitaxel in Stage Ivb, Recurrent or Persistent Cervical Cancer. *Gynecol. Oncol.* **2007**, *105*, 299−303.

(11) Hayashi, T.; Yoshizawa, M.; Watanabe, N.; Murayama, Y.; Shimizu, H. A Case of Recurrent Gastric Cancer Effectively Treated by Combined Chemotherapy of Weekly Paclitaxel (PTX) and CDDP. *Gan to Kagaku Ryoho* **2006**, *33*, 1167−1169.

(12) Hu, X.; Wang, B.; Sun, S.; Tang, L.; Zhang, J.; Lv, F.; Wang, Z.; Wang, L.; Zhang, Q.; Zheng, C.; Qiu, L.; Jia, Z.; Lu, Y.; Liu, G.; Shao, Z. M. Cisplatin Improves Antitumor Activity of Weekly Nab-Paclitaxel in Patients with Metastatic Breast Cancer. *Int. J. Nanomed.* **2014**, *9*, 1443−1451.

(13) Tang, L. C.; Wang, B. Y.; Sun, S.; Zhang, J.; Jia, Z.; Lu, Y. H.; Di, G. H.; Shao, Z. M.; Hu, X. C. Higher Rate of Skin Rash in a Phase Ii Trial with Weekly Nanoparticle Albumin-Bound Paclitaxel and Cisplatin Combination in Chinese Breast Cancer Patients. *BMC Cancer* **2013**, *13*, 232−237.

(14) Huang, J.; Zhou, Y.; Zhang, H.; Qu, T.; Mao, Y.; Zhu, H.; Quan, L.; Xing, P.; Wang, J.; He, J.; Xu, N.; Sun, Y. A Phase Ii Study of Biweekly Paclitaxel and Cisplatin Chemotherapy for Recurrent or Metastatic Esophageal Squamous Cell Carcinoma: Ercc1 Expression Predicts Response to Chemotherapy. *Med. Oncol.* **2013**, *30*, 343−348.

(15) Jung, Y.; Lippard, S. J. Direct Cellular Responses to Platinum-Induced DNA Damage. *Chem. Rev.* **2007**, *107*, 1387−1407.

(16) Marrache, S.; Pathak, R. K.; Dhar, S. Detouring of Cisplatin to Access Mitochondrial Genome for Overcoming Resistance. *Proc. Natl. Acad. Sci. U.S.A.* **2014**, *111*, 10444−10449.

(17) Yoong, S. L.; Wong, B. S.; Zhou, Q. L.; Chin, C. F.; Li, J.; Venkatesan, T.; Ho, H. K.; Yu, V.; Ang, W. H.; Pastorin, G. Enhanced Cytotoxicity to Cancer Cells by Mitochondria-Targeting Mwcnts Containing Platinum(IV) Prodrug of Cisplatin. *Biomaterials* **2014**, *35*, 748−759.

(18) Mallick, A.; More, P.; Syed, M. M. K.; Basu, S. Nanoparticle-Mediated Mitochondrial Damage Induces Apoptosis in Cancer. *ACS Appl. Mater. Interfaces* **2016**, *8*, 13218−13231.

(19) Davoodi, P.; Ng, W. C.; Srinivasan, M. P.; Wang, C.-H. Codelivery of Anti-Cancer Agents Via Double-Walled Polymeric Microparticles/Injectable Hydrogel: A Promising Approach for Treatment of Triple Negative Breast Cancer. *Biotechnol. Bioeng.* **2017**, *114*, 2931.

(20) Vanhoefer, U.; Harstrick, A.; Wilke, H.; Schleucher, N.; Walles, H.; Schröder, J.; Seeber, S. Schedule-Dependent Antagonism of Paclitaxel and Cisplatin in Human Gastric and Ovarian Carcinoma Cell Lines in Vitro. *Eur. J. Cancer* **1995**, *31*, 92−97.

(21) Singla, A. K.; Garg, A.; Aggarwal, D. Paclitaxel and Its Formulations. *Int. J. Pharm.* **2002**, *235*, 179−192.

(22) Jones, N. A.; Turner, J.; McIlwrath, A. J.; Brown, R.; Dive, C. Cisplatin- and Paclitaxel-Induced Apoptosis of Ovarian Carcinoma Cells and the Relationship between Bax and Bak up-Regulation and the Functional Status of P53. *Mol. Pharmacol.* **1998**, *53*, 819−826.

(23) Ivanov, A. I.; Christodoulou, J.; Parkinson, J. A.; Barnham, K. J.; Tucker, A.; Woodrow, J.; Sadler, P. J. Cisplatin Binding Sites on Human Albumin. *J. Biol. Chem.* **1998**, *273*, 14721−14730.

(24) Xiao, H.; Song, H.; Yang, Q.; Cai, H.; Qi, R.; Yan, L.; Liu, S.; Zheng, Y.; Huang, Y.; Liu, T.; Jing, X. A Prodrug Strategy to Deliver

Cisplatin(IV) and Paclitaxel in Nanomicelles to Improve Efficacy and Tolerance. *Biomaterials* **2012**, *33*, 6507−6519.
(25) Desale, S. S.; Cohen, S. M.; Zhao, Y.; Kabanov, A. V.; Bronich, T. K. Biodegradable Hybrid Polymer Micelles for Combination Drug Therapy in Ovarian Cancer. *J. Controlled Release* **2013**, *171*, 339−348.
(26) Cai, L.; Xu, G.; Shi, C.; Guo, D.; Wang, X.; Luo, J. Telodendrimer Nanocarrier for Co-Delivery of Paclitaxel and Cisplatin: A Synergistic Combination Nanotherapy for Ovarian Cancer Treatment. *Biomaterials* **2015**, *37*, 456−468.
(27) Desale, S. S.; Soni, K. S.; Romanova, S.; Cohen, S. M.; Bronich, T. K. Targeted Delivery of Platinum-Taxane Combination Therapy in Ovarian Cancer. *J. Controlled Release* **2015**, *220*, 651−659.
(28) Liu, B.; Han, L.; Liu, J.; Han, S.; Chen, Z.; Jiang, L. Co-Delivery of Paclitaxel and Tos-Cisplatin Via Tat-Targeted Solid Lipid Nanoparticles with Synergistic Antitumor Activity against Cervical Cancer. *Int. J. Nanomed.* **2017**, *12*, 955−968.
(29) Moon, H. J.; Ko, D. Y.; Park, M. H.; Joo, M. K.; Jeong, B. Temperature-Responsive Compounds as in Situ Gelling Biomedical Materials. *Chem. Soc. Rev.* **2012**, *41*, 4860−4883.
(30) Vermonden, T.; Censi, R.; Hennink, W. E. Hydrogels for Protein Delivery. *Chem. Rev.* **2012**, *112*, 2853−2888.
(31) Wu, Y.-L.; Wang, H.; Qiu, Y.-K.; Liow, S. S.; Li, Z.; Loh, X. J. Phb-Based Gels as Delivery Agents of Chemotherapeutics for the Effective Shrinkage of Tumors. *Adv. Healthcare Mater.* **2016**, *5*, 2679−2685.
(32) Qu, Y.; Chu, B. Y.; Peng, J. R.; Liao, J. F.; Qi, T. T.; Shi, K.; Zhang, X. N.; Wei, Y. Q.; Qian, Z. Y. A Biodegradable Thermo-Responsive Hybrid Hydrogel: Therapeutic Applications in Preventing the Post-Operative Recurrence of Breast Cancer. *NPG Asia Mater.* **2015**, *7*, No. e207.
(33) Davoodi, P.; Ng, W. C.; Yan, W. C.; Srinivasan, M. P.; Wang, C.-H. Double-Walled Microparticles-Embedded Self-Cross-Linked, Injectable, and Antibacterial Hydrogel for Controlled and Sustained Release of Chemotherapeutic Agents. *ACS Appl. Mater. Interfaces* **2016**, *8*, 22785−22800.
(34) Wu, X.; He, C.; Wu, Y.; Chen, X. Synergistic Therapeutic Effects of Schiffs Base Cross-Linked Injectable Hydrogels for Local Co-Delivery of Metformin and 5-Fluorouracil in a Mouse Colon Carcinoma Model. *Biomaterials* **2016**, *75*, 148−162.
(35) Zhang, Z.-Q.; Song, S.-C. Thermosensitive/Superparamagnetic Iron Oxide Nanoparticle-Loaded Nanocapsule Hydrogels for Multiple Cancer Hyperthermia. *Biomaterials* **2016**, *106*, 13−23.
(36) Seo, B.-B.; Koh, J.-T.; Song, S.-C. Tuning Physical Properties and Bmp-2 Release Rates of Injectable Hydrogel Systems for an Optimal Bone Regeneration Effect. *Biomaterials* **2017**, *122*, 91−104.
(37) Buwalda, S. J.; Vermonden, T.; Hennink, W. E. Hydrogels for Therapeutic Delivery: Current Developments and Future Directions. *Biomacromolecules* **2017**, *18*, 316−330.
(38) Shinde, U. P.; Moon, H. J.; Ko, D. Y.; Jung, B. K.; Jeong, B. Control of Rhgh Release Profile from PEG−PAF Thermogel. *Biomacromolecules* **2015**, *16*, 1461−1469.
(39) Xu, X.; Huang, Z.; Huang, Z.; Zhang, X.; He, S.; Sun, X.; Shen, Y.; Yan, M.; Zhao, C. Injectable, NIR/pH-Responsive Nanocomposite Hydrogel as Long-Acting Implant for Chemophotothermal Synergistic Cancer Therapy. *ACS Appl. Mater. Interfaces* **2017**, *9*, 20361−20375.
(40) Lee, Y.; Choi, K.-H.; Park, K. M.; Lee, J.-M.; Park, B. J.; Park, K. D. In Situ Forming and H_2O_2-Releasing Hydrogels for Treatment of Drug-Resistant Bacterial Infections. *ACS Appl. Mater. Interfaces* **2017**, *9*, 16890−16899.
(41) Yu, L.; Ding, J. Injectable Hydrogels as Unique Biomedical Materials. *Chem. Soc. Rev.* **2008**, *37*, 1473−1481.
(42) Seo, H. W.; Kim, D. Y.; Kwon, D. Y.; Kwon, J. S.; Jin, L. M.; Lee, B.; Kim, J. H.; Min, B. H.; Kim, M. S. Injectable Intratumoral Hydrogel as 5-Fluorouracil Drug Depot. *Biomaterials* **2013**, *34*, 2748−2757.
(43) Ma, H.; He, C.; Cheng, Y.; Li, D.; Gong, Y.; Liu, J.; Tian, H.; Chen, X. Plk1shrna and Doxorubicin Co-Loaded Thermosensitive PLGA-PEG-PLGA Hydrogels for Osteosarcoma Treatment. *Biomaterials* **2014**, *35*, 8723−8734.
(44) Ma, H.; He, C.; Cheng, Y.; Yang, Z.; Zang, J.; Liu, J.; Chen, X. Localized Co-Delivery of Doxorubicin, Cisplatin, and Methotrexate by Thermosensitive Hydrogels for Enhanced Osteosarcoma Treatment. *ACS Appl. Mater. Interfaces* **2015**, *7*, 27040−27048.
(45) Petit, A.; Sandker, M.; Müller, B.; Meyboom, R.; van Midwoud, P.; Bruin, P.; Redout, E. M.; Versluijs-Helder, M.; van der Lest, C. H. A.; Buwalda, S. J.; de Leede, L. G. J.; Vermonden, T.; Kok, R. J.; Weinans, H.; Hennink, W. E. Release Behavior and Intra-Articular Biocompatibility of Celecoxib-Loaded Acetyl-Capped PCLA-PEG-PCLA Thermogels. *Biomaterials* **2014**, *35*, 7919−7928.
(46) Cho, H.; Kwon, G. S. Thermosensitive Poly-(D,L-Lactide-co-Glycolide)-Block-Poly(Ethylene Glycol)-Block-Poly-(D, L-Lactide-co-Glycolide) Hydrogels for Multi-Drug Delivery. *J. Drug Targeting* **2014**, *22*, 669−677.
(47) Petit, A.; Redout, E. M.; van de Lest, C. H.; de Grauw, J. C.; Müller, B.; Meyboom, R.; van Midwoud, P.; Vermonden, T.; Hennink, W. E.; van Weeren, P. R. Sustained Intra-Articular Release of Celecoxib from in Situ Forming Gels Made of Acetyl-Capped PCLA-PEG-PCLA Triblock Copolymers in Horses. *Biomaterials* **2015**, *53*, 426−436.
(48) Cho, H.; Gao, J.; Kwon, G. S. PEG-b-PLA Micelles and PLGA-b-PEG-b-PLGA Sol-Gels for Drug Delivery. *J. Controlled Release* **2016**, *240*, 191−201.
(49) Liu, Y.; Chen, X.; Li, S.; Guo, Q.; Xie, J.; Yu, L.; Xu, X.; Ding, C.; Li, J.; Ding, J. Calcitonin-Loaded Thermosensitive Hydrogel for Long-Term Antiosteopenia Therapy. *ACS Appl. Mater. Interfaces* **2017**, *9*, 23428−23440.
(50) Wu, Z.; Zou, X.; Yang, L.; Lin, S.; Fan, J.; Yang, B.; Sun, X.; Wan, Q.; Chen, Y.; Fu, S. Thermosensitive Hydrogel Used in Dual Drug Delivery System with Paclitaxel-Loaded Micelles for in Situ Treatment of Lung Cancer. *Colloids Surf., B* **2014**, *122*, 90−98.
(51) Shen, W.; Luan, J.; Cao, L.; Sun, J.; Yu, L.; Ding, J. Thermogelling Polymer−Platinum(IV) Conjugates for Long-Term Delivery of Cisplatin. *Biomacromolecules* **2015**, *16*, 105−115.
(52) Wang, W.; Deng, L.; Liu, S.; Li, X.; Zhao, X.; Hu, R.; Zhang, J.; Han, H.; Dong, A. Adjustable Degradation and Drug Release of a Thermosensitive Hydrogel Based on a Pendant Cyclic Ether Modified Poly(ε-Caprolactone) and Poly(Ethylene Glycol) Copolymer. *Acta Biomater.* **2012**, *8*, 3963−3973.
(53) Kolishetti, N.; Dhar, S.; Valencia, P. M.; Lin, L. Q.; Karnik, R.; Lippard, S. J.; Langer, R.; Farokhzad, O. C. Engineering of Self-Assembled Nanoparticle Platform for Precisely Controlled Combination Drug Therapy. *Proc. Natl. Acad. Sci. U.S.A.* **2010**, *107*, 17939−17944.
(54) Yang, J.; Liu, W.; Sui, M.; Tang, J.; Shen, Y. Platinum (IV)-Coordinate Polymers as Intracellular Reduction-Responsive Backbone-Type Conjugates for Cancer Drug Delivery. *Biomaterials* **2011**, *32*, 9136−9143.
(55) Xiao, H.; Qi, R.; Liu, S.; Hu, X.; Duan, T.; Zheng, Y.; Huang, Y.; Jing, X. Biodegradable Polymer - Cisplatin(IV) Conjugate as a Pro-Drug of Cisplatin(II). *Biomaterials* **2011**, *32*, 7732−7739.
(56) Luan, J.; Cui, S.; Wang, J.; Shen, W.; Yu, L.; Ding, J. Positional Isomeric Effects of Coupling Agents on the Temperature-Induced Gelation of Triblock Copolymer Aqueous Solutions. *Polym. Chem.* **2017**, *8*, 2586−2597.
(57) Aryal, S.; Hu, C.-M. J.; Zhang, L. F. Polymer−Cisplatin Conjugate Nanoparticles for Acid-Responsive Drug Delivery. *ACS Nano* **2010**, *4*, 251−258.
(58) Chen, Y.; Luan, J.; Shen, W.; Lei, K.; Yu, L.; Ding, J. Injectable and Thermosensitive Hydrogel Containing Liraglutide as a Long-Acting Antidiabetic System. *ACS Appl. Mater. Interfaces* **2016**, *8*, 30703−30713.
(59) Chen, Y.; Li, Y.; Shen, W.; Li, K.; Yu, L.; Chen, Q.; Ding, J. Controlled Release of Liraglutide Using Thermogelling Polymers in Treatment of Diabetes. *Sci. Rep.* **2016**, *6*, 31593.
(60) Hong, J. H.; Lee, H. J.; Jeong, B. Injectable Polypeptide Thermogel as a Tissue Engineering System for Hepatogenic Differentiation of Tonsil-Derived Mesenchymal Stem Cells. *ACS Appl. Mater. Interfaces* **2017**, *9*, 11568−11576.

DOI: 10.1021/acsami.7b11998
ACS Appl. Mater. Interfaces 2017, 9, 40031−40046

(61) Dash, S.; Murthy, P. N.; Nath, L.; Chowdhury, P. Kinetic Modeling on Drug Release from Controlled Drug Delivery Systems. *Acta Pol. Pharm.* **2010**, *67*, 217−223.
(62) Zhang, L.; Shen, W.; Luan, J.; Yang, D.; Wei, G.; Yu, L.; Lu, W.; Ding, J. Sustained Intravitreal Delivery of Dexamethasone Using an Injectable and Biodegradable Thermogel. *Acta Biomater.* **2015**, *23*, 271−281.
(63) Chou, T.-C.; Talalay, P. Quantitative Analysis of Dose-Effect Relationships: The Combined Effects of Multiple Drugs or Enzyme Inhibitors. *Adv. Enzyme Regul.* **1984**, *22*, 27−55.
(64) Wang, W.; Liu, J.; Li, C.; Zhang, J.; Liu, J.; Dong, A.; Kong, D. Real-Time and Non-Invasive Fluorescence Tracking of in Vivo Degradation of the Thermosensitive PEGlyated Polyester Hydrogel. *J. Mater. Chem. B* **2014**, *2*, 4185−4192.
(65) Chen, L.; Ci, T.; Yu, L.; Ding, J. Effects of Molecular Weight and Its Distribution of PEG Block on Micellization and Thermogellability of PLGA−PEG−PLGA Copolymer Aqueous Solutions. *Macromolecules* **2015**, *48*, 3662−3671.

DOI: 10.1021/acsami.7b11998
ACS Appl. Mater. Interfaces 2017, 9, 40031−40046